学位論文

The role of Thy1$^+$ cells in fibrogenesis during mouse chronic liver injury
(マウス慢性肝障害時の線維質形成における Thy1$^+$ 細胞の役割)

平成 28 年 12 月博士(理学) 申請

東京大学大学院理学系研究科
生物科学専攻
勝又　廉

Table of Contents

List of Abbreviations

αSMA: Alpha smooth muscle actin

BD: Bile duct

BDL: Bile duct ligation

BECs: Biliary epithelial cells

CCl_4: Carbon tetrachloride

CK19: Cytokeratin 19

CV: Central vein

DDC: 3,5-diethoxycarbonyl-1,4-dihydrocollidine

ECM: Extracellular matrix

EdU: 5-ethynyl-2 deoxyuridine

EpCAM: Epithelial cell adhesion molecule

GFAP: Glial fibrillary acidic protein

GFP: Green fluorescent protein

HA: Hepatic artery

HSCs: Hepatic stellate cells

Lrat: Lecithin-retinol acyltransferase

LSECs: Liver sinusoidal endothelial cells

NPCs: Non-parenchymal cells

NTPDase2: Ectonucleoside triphosphate diphosphohydrolase 2

PDGFRα: Platelet-derived growth factor receptor alpha

PDGFRβ: Platelet-derived growth factor receptor beta

PV: Portal vein

Sca-1: Stem cells antigen-1

Stab2: Stabillin-2

TAA: Thioacetamide

TCRβ chain: T cell receptor beta chain

Thy1: Thymus cell antigen-1

Thy1 MCs: Thy1-expressing mesenchymal cells

Abstract

Liver fibrosis, a condition that is characterized by excessive production and accumulation of extracellular matrix (ECM), including collagen, is the most common outcome of chronic liver injuries of different etiologies. Vitamin A storing hepatic stellate cells (HSCs) are considered to be the main source of this collagen production upon activation in response to liver injury. In contrast, the contribution of other cell types to this fibrogenic response remains largely elusive, due to the lack of specific surface markers to identify and isolate these cells for detailed analysis. The present study identifies a mesenchymal population of $Thy1^+$ $CD45^-$ cells (Thy1 MCs) in the mouse liver, which reside near the portal vein *in vivo* and indicate pro-fibrogenic characteristics *in vitro*, shown by their expression of collagen and α-smooth muscle actin. Flow cytometric analysis of mouse liver non-parenchymal cells revealed that vitamin A storage and Thy1 expression were mutually exclusive, indicating that Thy1 MCs are distinct from HSCs. Importantly, Thy1 MCs reacted and contributed to the development of liver fibrosis specifically in mouse models of cholestatic liver injury. Upon cholestatic liver injury, collagen-producing Thy1 MCs expanded in cell number and inhibited collagen degradation through upregulation of matrix metalloproteinase inhibitor *Timp1* expression, thereby promoting the accumulation of ECM in the peri-portal area. *Conclusion:* The present study establishes Thy1 as a useful cell surface

marker to prospectively identify and isolate peri-portal fibroblasts, and further highlights a significant contribution of these cells to the pathogenesis of liver fibrosis caused by cholestatic liver injuries. Thy1 MCs may be an interesting therapeutic target for treating liver fibrosis, in addition to the well-characterized HSCs.

Introduction

The structure and function of the liver

The liver is the central organ for homeostasis of a living organism, and it serves various roles in metabolism and detoxification. The liver mainly consists of parenchymal cells, or hepatocytes, which serve practical metabolic functions, and occupy about 80% of the liver volume. Other cells called non-parenchymal cells (NPCs), which only contribute to about 6.5% of the liver volume, compose about 40% of the total number of liver cells[1], indicating that NPCs may play physiological roles in maintaining tissue homeostasis. These non-parenchymal cells contain, biliary epithelial cells (BECs), portal fibroblast (PFs), liver sinusoidal endothelial cells (LSECs), hepatic stellate cells (HSCs), Kupffer cells, immune cells, and mesothelial cells (Figure 1). BECs compose the bile duct, which serves to excrete bile that is produced by hepatocytes. PFs are fibroblasts that reside near the bile duct and portal vein, within the portal mesenchyme called the “Glisson’s capsule”, and their specific roles in liver physiology are unclear. LSECs compose the vascular structure called the sinusoid, and also serve as a filter of substances supplied to hepatocytes. HSCs line the walls of the sinusoids, a space between hepatocytes called the “space of Disse”, and serve as vitamin A storing cells. Kupffer cells are tissue-resident macrophages, which are found in the luminal side of the endothelium, and serve various roles in maintaining tissue homeostasis along with

other immune cells. Mesothelial cells together compose the mesothelium that encapsulate the liver body and serve important roles in liver development and regeneration from injury. Until recently, the liver was rather considered as a simple organ that is composed mostly of parenchymal cells, or hepatocytes, and NPCs have achieved less attention. However instead, the liver consists of various cell types as mentioned above, and the intrinsic interactions of these cells are essential in maintaining liver homeostasis.

The structural and functional unit of the liver can be delineated into a hexagonal structure called the "lobule" (Figure 1), which consists of three zones: zone 1 (the peri-portal area), zone 2 (the "transitional" parenchyma), and zone 3 (the peri-central area). The portal area contains the portal triad that consists of the portal vein, bile duct, and hepatic artery. The portal triad is encapsulated in a mesenchymal tissue called the Glisson's capsule. Nutrients from food intake and drugs absorbed through the gastrointestinal tract are supplied into blood flow, and they enter the liver system through the portal vein. Once in the liver system, the blood flows through the sinusoid, supplying nutrients and other substances to hepatocytes, and exits out of the central vein. Hepatocytes that spread radially from the portal vein are non-uniform in their metabolic functions depending on the zone they are located in. Since oxygen-rich blood enters the liver through the hepatic artery located near the portal vein, it is reasonable that zone 1 hepatocytes are specialized for oxidative liver functions such as gluconeogenesis, β-oxidation of

fatty acids and cholesterol synthesis. Whereas on the other hand, zone 3 hepatocytes are more specialized for glycolysis, lipogenesis and cytochrome P-450-based drug detoxification[2] owing to the difference in expression of metabolic enzymes. Due to the frequent influx of foreign substances into the liver system, the liver is prone to damage, and different zones of the liver parenchyma are susceptible to different insults owing to their metabolic functions.

Liver injury and pathogenesis

The liver is renowned for its highly remarkable regenerative capacities and can compensate for injuries caused by various insults, such as viral infection, metabolic disorders, chemical and toxic stresses. Liver injuries often result in the death and loss of hepatocytes, where there is temporal compensatory synthesis of extracellular matrix (ECM) by a special set of collagen-producing cells called "myofibroblasts", to provide mechanical stability and scaffold that is beneficial for hepatic regeneration. In acute liver injuries, when the damage and fibrous stimuli subside, deposited collagen eventually dissolves, rendering the liver back into its normal state by means of natural healing. However, in cases of chronic liver injuries, where damage and fibrous stimuli persist, there is excessive production and decreased degradation of ECM, together contributing to its accumulation that eventually leads to liver fibrosis and cirrhosis[3] (Figure 2). This alters hepatic functions, hence causing organ failure and dysfunction.

Cell types that contribute to pathogenesis of liver fibrosis

Hepatic stellate cells (HSCs) are one of the mesenchymal-type cell populations within the liver and are well known to play a central role in collagen synthesis upon liver injury[4]. Under normal conditions, HSCs serve as vitamin A storing cells that exhibit characteristics of pericytes existing in the space of Disse, and line the hepatic sinusoid[5]. HSCs are usually defined by their expression of desmin, glial fibrillary acidic protein (GFAP), cytoglobin, and lecithin-retinol acyltransferase (Lrat). They are thought to be "quiescent" in the normal state, and become "activated" upon injury to the liver, differentiating into fibrogenic myofibroblasts that are responsible for synthesis and deposition of collagen in areas of damage[6]. Hence, HSCs are regarded as myofibroblast precursors, making them the center of attention as a therapeutic target in liver fibrosis.

In addition to HSCs, other cell populations including portal fibroblasts, bone marrow-derived fibrocytes, and mesothelial cells have been suggested as alternative sources of collagen in the injured liver[7-10]. Among these populations, portal fibroblasts (PFs) have been well documented to play a role as myofibroblast precursors, particularly in conditions of biliary fibrosis caused by cholestatic liver injury[11,12]. PFs are defined as a non-HSC fibroblast population that can be found in the periportal mesenchyme surrounding the bile ducts, with the notion that they are a heterogeneous population[13]. PFs are usually distinguished from HSCs by their expression of elastin, fibulin-2, type XV collagen, and ectonucleoside

triphosphate diphosphohydrolase 2 (NTPDase2). However, studies on PFs up until today have depended on isolation methods based on outgrowth from dissected bile-segments[14], size-selection[15], and marker negative flow cytometry-based exclusion of non-HSC-derived myofibroblasts[16]. None of these methods identify or isolate PFs by positive selection, thus hampering accurate evaluation of the cell population of interest.

Typically, cell types that constitute the liver have been characterized by their morphology, histological location, and expression of specific markers observed by immunohistochemistry. Although histology is a powerful tool in performing diagnosis and elucidating the relevance of cells to tissue abnormality and diseases, there are limits as to analyzing the specific physiological roles of these cells without means to isolate them. Meanwhile, flow cytometry is a powerful tool in performing quantitative and qualitative analysis, and a high-throughput characterization and identification of various cell types, all within a single preparation. In addition, isolation of specific cell types by flow cytometry is easily achievable by identification of cells by specific cell surface markers. Not until recently was flow cytometry-based isolation and characterization of various cell types of liver-constituting cells implemented for cellular and molecular analysis. Various cell surface markers that specifically identify liver-constituting cells have been established since then, such as EpCAM for BECs[17], Stab2 for LSECs[18], and mesothelin for mesothelial cells[19]. Although, a specific cell surface marker for

HSCs has not been identified, the high abundance of retinoid (vitamin A)-storing lipid droplets makes it possible to detect their autofluorescence using a UV laser. Specific isolation of these cells using a cell sorter allowed detailed analysis of their cellular properties and their physiological roles in the developing liver and chronically injured liver. However, up to date, a specific cell surface marker for PFs has not been identified, and isolation methods depend on exclusion of HSCs from collagen-reporter mice[20,21], which mark collagen-producing cells. Therefore, identification of a specific cell surface marker that distinguishes PFs from HSCs is essential for the evaluation of their physiological roles in liver pathology.

Besides the fibrotic responses upon chronic liver injury, there also is thought to be a putative stem/progenitor cell-mediated regenerative response. This is achieved when the liver faces an intolerable level of damage, where hepatocyte proliferation is hampered, and a putative population of liver stem/progenitor cells is posited to become activated to repopulate the damaged tissue, originating from the peri-portal area[22]. Rigorous efforts have been put into identification of such stem cell population by search for cell surface markers, although its exact existence is still under debate[23]. Among those markers, Thy1 (Thymus cell antigen-1, or CD90) was reported as a marker for "oval cells," another name for liver stem/progenitor cells, in chronically injured rat liver[23]. Thy1 is a glycophosphatidylinositol anchored cell surface protein, which is widely used as a stem cell marker, expressed in hematopoietic stem cells and mesenchymal stem cells. However, later studies

revealed that Thy1 is not a marker for oval cells, but rather a marker for cells that reside in close proximity to oval cells, constituting a "stem cell niche[25]".

It has been previously reported that in mouse models of chronic liver injury, peri-portal Thy1-expressing cells constitute the putative niche for liver stem/progenitor cells via paracrine signaling of fibroblast growth factor 7, thereby contributing to liver stem/progenitor cell-mediated regeneration[25]. It has been also described in rats that Thy1-expressing cells in the stem cell niche compartment behave as activated mesenchymal-epithelial cells *in vitro*, presumably acting as progenitor cells themselves[26,27]. Subsequently, Thy1 was reported to be a marker of liver myofibroblast, residing near the portal vein[28-30]. These reports all identify a peri-portal mesenchymal population of Thy1-expressing cells that could potentially be the equivalent of PFs, which lacked a definitive marker for isolation and subsequent analysis. The use of Thy1 as a PF marker has not been empirically validated, nor has it been essentially understood as to whether and how Thy1-expressing cells contribute to the pathogenesis of liver fibrosis *in vivo*.

In the present study, in aim to reveal the regenerative role of peri-portal Thy1-expressing cells upon mouse liver injury, detailed characterization of these cells were performed. Of the Thy1-expressing cells, a leukocyte marker CD45 negative subpopulation with characteristics of mesenchymal cells localized in the peri-portal area and displayed key characteristics of collagen producing

myofibroblasts, while being distinct from the well-established myofibroblast precursor HSCs. These cells specifically expressed representative markers of PFs, thus indicating that cell surface expression of Thy1 and CD45 is useful in identifying PFs. Furthermore, as a representative population of PFs, Thy1 MCs act as an alternative source of collagen deposition in the injured liver, specifically in cholestatic injury, thereby contributing to the pathogenesis of liver fibrosis in addition to conventional HSCs.

Materials and Methods

Animals and liver injury models

Wild-type C57BL/6J mice were purchased from CLEA Japan, Inc. GFP transgenic mice were kindly provided by Dr. M. Okabe (Osaka University). All animals were maintained under specific pathogen free conditions. All animal experiments were conducted in accordance with the Guideline for the Care and Use of Laboratory Animals of The University of Tokyo, under the approval of the Institutional Animal Care and Use Committee of Institute of Molecular and Cellular Biosciences, The University of Tokyo (approval numbers 2501, 2501-1, 2609, 2706 and 2804). For cholestatic liver injury models, mice were fed with diet containing 0.1% 3,5-diethoxycarbonyl-1,4-dihydrocollidine (DDC; F-4643, Bio-serv), or common bile duct ligation (BDL) was performed using standard techniques[31]. For hepato-toxic liver injury models, mice were injected with carbon tetrachloride (CCl_4; 039-01276; Wako; 1 mL/kg body weight dissolved in corn oil) intraperitoneally 2 times per week, or thioacetamide (TAA; 204-00881; Wako; 300 mg/L) were supplemented in drinking water. The duration of each injury model is indicated in the figure legends.

Histological analysis

Livers were dissected out from the peritoneum of mice euthanized by cervical dislocation. The left lobe was cut in a perpendicular axis relative to the large

portal vein running in the lobe, which results in a crescent form block, and was used for all analysis. Dissected livers were either pre-fixed in Zamboni's Fixative at 4°C over night or directly embedded in Tissue-Tek O.C.T. Compound (4583, Sakura Finetek USA, Inc.) and snap frozen in liquid nitrogen. Frozen sections (thickness 8 µm) from the liver were placed on APS-coated glass slides (Matsunami Glass) using a HM525 cryostat (Thermo Scientific). Samples directly embedded in O.C.T. after liver dissection were either fixed in acetone for more than 3 hours at 4°C or 4% paraformaldehyde for 10 minutes at room temperature after sectioning. After blocking in 5% skim milk/PBS for 30 minutes at room temperature, the samples were incubated with primary antibodies at 4°C over night and then, if necessary, with fluorescence-conjugated secondary antibodies for 2 hours at room temperature after washing with PBS for 10 minutes while shaking. Antibodies and their used concentrations in the present study are listed in Table 1. EdU was detected using Click-iT® Plus EdU Alexa Fluor 488 Imaging kit (Life technologies), following the manufacturer's instructions. Nuclei were counterstained with Hoechst 33342 for 5 minutes at room temperature. Fluoromount (Diagnostic BioSystems) was mounted on tissue sections to avoid fading of fluorescence, and covered with cover slips (MATSUNAMI). Liver sections were imaged with fluorescence microscope (Axio Observer.Z1; Zeiss) and confocal microscope (FV3000; Olympus). For the quantification of Thy1 positive areas, immunostained liver sections were imaged and quantified using the IN Cell Analyzer 2000 and IN Cell Developer (GE Healthcare). In brief, the outline of Thy1 positive signals was quantified by their

signal intensity to determine Thy1 positive area. The actual images were observed to determine the threshold of Thy1 positive signal. Small signals of T-lymphocytes were removed from area quantification by kernel size selection. Whole liver area was determined by tracing the outline of nuclear signals at the perimeter of liver sections. Holes formed by portal vein and central vein were removed from whole liver area quantification.

RNA extraction and gene expression analysis

Total RNA was extracted from whole liver chunks and cultured/sorted cells using Trizol reagent (Invitrogen) and treated with DNase I (Invitrogen), following the manufacturer's instructions. Whole liver chunks were homogenized, or cells were suspended in Trizol, and chloroform was added at a ratio of 0.2:1.0 to the initial amount of Trizol used for sample suspension. The mixture was briefly vortexed and samples were centrifuged at 12,000 x g for 15 minutes at 4°C. The aqueous phase of the mixture that contains RNA was transferred to a fresh tube, and 10 μg of glycogen and 0.5 mL of isopropyl alcohol was added. The mixture was briefly vortexed and centrifuged at 12,000 x g for 10 minutes at 4°C. After removing the supernatant, the pellet was washed with 75% ethanol. Samples were centrifuged at 12,000 x g for 5 minutes at 4°C. After removing the supernatant, RNA pellet was briefly dried at room temperature. RNA pellet was resuspended in RNase-free water. NucleoSpin® RNA XS kit (MACHEREY-NAGEL) was used for cells of low yield, following the manufacture's instructions. After DNase treatment

for 15 minutes at room temperature, 2.5 μmol of EDTA was added for inactivation and heated at 65°C for 10 minutes. Resulting total RNA was used for cDNA synthesis with PrimeScript™ RT Master Mix (TaKaRa). Quantitative RT-PCR analyses were performed using LightCycler 96 (Roche) with SYBR Premix Ex Taq (TaKaRa). Primers were added to the reaction mixture so that the final concentration would be 0.4 μM. Expression of β-actin (*Actb*) was used as an internal control for all expression analysis, which was confirmed to be unchanged between normal and injured conditions. Primer sequences are listed in Table 2.

Cell preparation and flow cytometry

A single-cell suspension from the mouse liver was obtained by a two-step collagenase perfusion method and used for preparation of hepatocytes and non-parenchymal cells (NPCs) by centrifugal separation, as described previously[17]. Livers were perfused via the portal vein with Liver Perfusion Medium (136 mM NaCl, 5.4 mM KCl, 0.7 mM NaH_2PO_4 $2H_2O$, 0.82 mM Na_2HPO_4 $12H_2O$, 10 mM HEPES, 4.2 mM $NaHCO_3$, 5 mM Glucose, 0.5 mM EGTA) at a flow rate of 3 mL/minute for 5 minutes. Then, the liver was perfused via the portal vein with basic perfusion solution (136 mM NaCl, 5.4 mM KCl, 0.5 mM $CaCl_2$, 0.5 mM NaH_2PO_4 $2H_2O$, 0.42 mM Na_2HPO_4 $12H_2O$, 10 mM HEPES, 4.2 mM $NaHCO_3$, 5 mM Glucose) containing 0.25 g/L collagenase (YAKULT) at a flow rate of 3 mL/minute for 7 minutes. Digested liver was transferred to a glass dish and chopped into small pieces using a surgical knife, in DMEM containing 10% FBS. Cells

dispersed by pipetting were passed through a 70 μm cell strainer and the flow through fraction was used for the next step as the first cell suspension. The undigested clot on the strainer was recovered and redigested with basic perfusion medium containing 0.25 g/L collagenase, 0.5 g/L pronase (Roche Diagnostics), and 0.25 g/L DNase I (Sigma) by stirring for 20 minutes at 37°C. This digested liver was also passed through a 70 μm cell strainer and the flow through was combined with the first cell suspension. After centrifugation at 100 x g for 2 minutes, the cell pellet was used as the hepatocyte fraction after Percoll (GE Healthcare) density centrifugation. On the other hand, the supernatant was transferred to a new tube and the centrifugation was repeated until no cell pellet was observed. The final supernatant was centrifuged at 300 x g for 5 minutes and the precipitated cells were used as the NPC fraction for flow cytometry. Aliquots of cells were blocked with anti-FcR antibody, costained with fluorescence- and/or biotin-conjugated antibodies (listed in Table 1), and then incubated with APC-conjugated streptavidin (BD Biosciences) if necessary. EdU was detected using Click-iT® Plus EdU Alexa Fluor 488 Cytometry Assay Kit (Life technologies), following the manufacturer's instructions. The samples were analyzed by FACSCanto II (BD Biosciences) or sorted by Moflo XDP (Beckman-Coulter). Dead cells were excluded by propidium iodide staining. HSCs were identified in flow cytometry based on vitamin A autofluorescence signal detected by violet laser at 405 nm. Data were analyzed on the FlowJo software.

Cell culture of Thy1-expressing cells and HSCs

After incubation of NPCs with the biotin-conjugated Thy1 antibody, followed by incubation with APC-conjugated streptavidin, cells were resuspended in autoMACS® Running Buffer (Miltenyi Biotech). Cell suspension was incubated with anti-APC microbeads (Miltenyi Biotech). Conjugated cells were separated using the autoMACS® Pro Separator (Miltenyi Biotech) using the possel-s protocol. Cells contained in the positively separated fraction were suspended in modified standard medium (William's medium E containing 10% FBS, 10 mM nicotinamide, 2 mM L-glutamine, 0.2 mM ascorbic acid, 20 mM HEPES pH 7.5, 1 mM sodium pyruvate, 17.6 mM $NaHCO_3$, 14 mM glucose, and 50 mg/mL gentamicin) and seeded on a cell culture dish. For HSC isolation, MACS negative cells were subjected to a density centrifugation containing 11% Histodenz (Sigma) at 1500 x g. Cells were incubated for 12 hrs in 37°C with 5% CO_2, and non-adhering cells were washed out. Media was changed every 2 to 3 days.

Mouse irradiation and bone marrow transplantation

Bone marrow cells were prepared by flushing tibias and femurs of donor GFP transgenic mice with cold PBS, which were collected and cells were resuspended in NH_4Cl buffer (16.5 mM Tris, 105mM NH_4Cl, pH 7.4), subjected to hemolysis on ice for 5 minutes to eliminate red blood cells. Cells were centrifuged at 300 x g, and the resulting pellet was used as bone marrow cells. Collected bone marrow cells (5.0×10^6 cells) were injected intravenously to recipient wild type mice, which had

been pre-exposed to a lethal dose of radiation of 9.5 Gy (M-150WE; Softex). The bone marrow-reconstituted mice were maintained for at least 1 month after transplantation before commencing DDC diet. Peripheral blood was collected at the timing of the experiment and was confirmed to be GFP positive (>80%) by flow cytometry.

Statistical analysis

Data are expressed as the mean ± S.E.M. (standard error of the mean). The results were assessed using a two-tailed Student's *t* test, unless otherwise noted. Comparison of gene expression in multiple liver cell fractions was done using one-way analysis of variance (ANOVA) with subsequent Tukey tests. Differences with *P* value less than 0.05 were considered statistically significant.

Results

Thy1-expresstion does not mark oval cells in the mouse liver

Thy1 has been previously reported as a marker for oval cells, and they were shown to expand in conditions of stem/progenitor cell mediated hepatic regeneration[24]. However, these histological analyses were solely performed in serial sections, which did not allow accurate evaluation of cell markers. Accordingly, immunostaining was performed for Thy1 and CK19, a marker for BECs which is also applied conveniently as a maker for oval cells, in normal and chronically injured mouse liver sections, followed by observation with confocal microscope to show their specific location. DDC diet-induced liver injury and TAA-induced liver injury were used as chronic liver injury models that induce stem/progenitor cell mediated hepatic regeneration. DDC inhibits the activity of ferrochelatase, an enzyme that catalyzes the insertion of ferrous iron into protoporphyrin IX[32], resulting in the accumulation of porphyrin-containing pigment plugs in the bile ducts, which ultimately cause cholestatis[33]. TAA is bioactivated mainly in zone 3 hepatocytes via oxidation processes owing to their high expression of metabolic enzymes, leading to generation of *S*-oxide and the highly reactive *S,S*-dioxide, which is presumably responsible for hepatotoxicity[34]. Chronic administration of these xenobiotics causes expansion of BECs, which also resembles the emersion of oval cells. No co-localization of Thy1 and CK19 was observed, but instead Thy1-expressing cells resided in close proximity to oval cells in both normal and

chronically injured mouse liver sections (Figure 3). To further confirm that Thy1-expressing cells are separate from oval cells, in addition to tissue analysis, flow cytometric analysis was performed of NPCs collected from normal and injured mouse livers. Flow cytometry allows identification of various cell types at single cell level by marking them with specific cell surface antigens. Oval cells are presumably included in EpCAM-expressing BECs[17]. As a result, Thy1-expressing cells and EpCAM-expressing BECs were mutually exclusive in both normal and chronically injured livers (Figure 4), thus confirming that Thy1-expressing cells in mouse liver are not oval cells at the cellular level as well.

Hepatic Thy1-expressing cells can be divided into two subpopulations

It has been previously reported that there are mesenchymal cells in the portal area that express the cell surface marker, Thy1 in mouse liver[25,26]. To characterize these Thy1-expressing cells, immunostaining of Thy1 and CD31, a marker of endothelial cells, was performed on normal mouse liver sections, to identify the anatomical location of these cells. As a result, Thy1 staining was prominent around the portal vein, while weaker and scattered staining in the parenchyma was confirmed as well (Figure 5A). Magnified images showed that most Thy1-expressing cells in the peri-portal region were elongated and planular (Figure 5B), resembling fibroblasts. These peri-portal Thy1-expressing cells also expressed desmin and the known PFs markers elastin and NTPDase2 (Figure 6), thus defining them as Thy1-expressing mesenchymal cells (or Thy1 MCs).

Vascular walls surrounding the portal vein were also positive for these markers. On the other hand, Thy1-expressing cells in the parenchyma were round and spherical, and existed within the luminal side of the endothelium (Figure 5B), together implying their identity as leukocytes.

Given the notion that Thy1 was originally identified as a thymocyte antigen and is known to be expressed on surfaces of various cell types, including fibroblasts and lymphocytes, Thy1-expressing cells were divided based on the expression of the leukocyte marker CD45 to distinguish between fibroblasts and lymphocytes. Accordingly, flow cytometric analysis was performed on NPCs collected from normal mouse liver, which revealed that Thy1-expressing cells could be divided into two distinct subpopulations based on CD45 expression (Figure 7A), namely, $Thy1^+$ $CD45^+$ leukocytes and $Thy1^+$ $CD45^-$ mesenchymal cells. $Thy1^+$ $CD45^+$ leukocytes also co-expressed CD3ε and TCR β chain (Figure 7B), confirming that these cells were mostly T lymphocytes. Subsequently, revisiting the previous immunohistochemical analysis, co-immunostaining of Thy1 and CD45 was performed, revealing that virtually all Thy1-expressing cells in the parenchyma co-expressed CD45, while most of Thy1-expressing cells in the peri-portal region did not (Figure 8). In other words, T lymphocytes were distributed throughout the liver tissue, while Thy1 MCs were exclusively localized in the peri-portal area.

Characterization of Thy1-expressing peri-portal mesenchymal cells

Thy1 has been suggested as a marker of portal (myo)fibroblasts, yet selective isolation and an in-depth characterization of these Thy1-expressing cells in mouse liver has not been performed[35]. Thus, in aim to evaluate the relationship of the present Thy1 MCs to portal (myo)fibroblasts, taking advantage of Thy1 as a surface antigen, $Thy1^+$ cells were isolated as a whole using a specific monoclonal antibody and magnetic-activated cell sorting. Subsequently, $Thy1^+$ cells were seeded on a culture dish, and non-adhering T lymphocytes were washed out after 12 hours of seeding. Five days after initial seeding, adhered cells showed fibroblastic morphology, represented by spindle-like shaped body and extended processes (Figure 9A). By flow cytometric analysis, adhered cells were confirmed to be mostly $Thy1^+$ and $CD45^-$ (Figure 10A). In addition, these cells were proliferative, shown by their incorporation of thymidine analogue EdU (Figure 10B). By 15 days after seeding, the cells progressively showed morphology of activated myofibroblasts, represented by gradual spreading and flattening accompanied by appearance of filamentous structures (Figure 9B). By immunostaining, in addition to Thy1-expression, these cells were confirmed to express type I collagen and alpha-smooth muscle actin (α-SMA) (Figure 11), which are representative characteristics of myofibroblasts. Quantitative gene expression analysis was performed to further represent their myofibroblastic characteristics (Figure 12). Expression of type I and type III collagen genes (*Col1a1* and *Col3a1*, respectively) gradually increased over a course of 3 weeks after initial culture, whereas expression of α-SMA (*Acta2*) did not change across the indicated time points. The

expression of *Thy1* and *Fgf7* were validated to assess that the isolated cells are the cells of interest[25]. Additionally, these cells expressed vimentin (*Vim*), confirming their identity as mesenchymal cells.

Thy1 MCs represent a distinct cell population from HSCs

Based on the myofibroblastic characteristics of Thy1 MCs upon culture, the similarities and differences between Thy1 MCs and HSCs were investigated, the latter of which is the best characterized myofibroblast precursor population of the liver. Thy1 MCs were isolated as mentioned above from normal mouse liver, and HSCs were subsequently collected from the remaining NPC flow through by density-gradient centrifugation owing to their abundance of retinoid (vitamin A)-storing lipid droplets[36]. Isolated Thy1 MCs contained no apparent lipid droplets, which on the contrary were characteristic to HSCs observed under the phase-contrast microscope (Figure 13A). After prolonged culture (10 days), HSCs gradually developed morphology of activated myofibroblasts, represented by gradual spreading and flattening accompanied by appearance of filamentous structures (Figure 13B), like Thy1 MCs. By immunostaining, these cells expressed type I collagen and α-SMA (Figure 14). These results show that Thy1 MCs and HSCs share similar characteristics as myofibroblast precursors *in vitro*, yet they can be clearly distinguished by Thy1 expression and lipid storage, respectively.

Flow cytometric analysis of NPCs of normal mouse liver revealed that vitamin A

autofluorescence and Thy1 expression were mutually exclusive (Figure 15A), thereby indicating that Thy1 MCs and HSCs are two distinctive myofibroblast precursor populations. Since flow cytometry-based analysis of Thy1-expression and vitamin A autofluorescence allowed to distinguish Thy1 MCs and HSCs, these two populations were further analyzed for several surface markers that are known to be expressed on mesenchymal and/or myofibroblastic cells (Figure 15B). Expression of CD73 was weaker in Thy1 MCs compared to HSCs, while that of CD105 was comparable between the two populations. Expression of CD146 was confirmed in both Thy1 MCs and HSCs, despite variable levels of expression in HSCs. HSCs expressed PDGFRα and PDGFRβ, whereas Thy1 MCs did not. On the other hand, Thy1 MCs expressed Sca-1, while its expression was low in HSCs. It is also worthy of note that HSCs apparently consisted of two subpopulations based on the expression of PDGFRα or CD146.

Flow cytometric analysis of NPCs of DDC and TAA injured mouse livers also revealed that vitamin A autofluorescence and Thy1 expression were mutually exclusive. Although, HSCs are known to lose their signature retinoid (vitamin A)-containing lipid droplets upon spontaneous "activation" into myofibroblast-like cells *in vitro*, HSCs *in vivo* are reported to retain these lipid droplets in their cellular body, even after liver injury and subsequent activation into myofibroblasts[37]. This allowed distinguishing HSCs from Thy1 MCs by vitamin A autofluorescence and Thy1-expression in NPCs prepared from injured mouse livers

as well (Figure 16A). To further characterize these two populations, the change in expression of surface markers that were investigated in the above section was analyzed. In DDC-induced liver injury, Thy1 MCs showed weak induction of PDGFRβ expression, whereas expression of CD146 decreased. HSCs did not show apparent change in marker expression, except $CD146^{low}$ and $PDGFR\alpha^{low}$ subpopulation seemed to have disappeared (Figure 16B). On the other hand, in TAA-induced liver injury, Thy1 MCs showed induction of PDGFRβ. While $CD146^{high}$ subpopulation of HSCs seemed to have disappeared (Figure 16C).

Also, gene expression profiling was performed by quantitative RT-PCR analysis within various cell populations that constitute the liver. Hepatocytes, BECs ($EpCAM^+$), Thy1 MCs ($EpCAM^-$ $Thy1^+$ $CD45^-$), T lymphocytes ($EpCAM^-$ $Thy1^+$ $CD45^+$), blood cells except T lymphocytes ($EpCAM^-$ $Thy1^-$ $CD45^+$), HSCs ($EpCAM^-$ $Thy1^-$ $CD45^-$ vitamin A^+), and others (All markers negative) were isolated from normal mouse liver, and evaluated for expression of reported signature genes of HSCs and PFs. Adequate cell isolation was confirmed by specific expression of each marker in the corresponding cell compartment (Figure 17). Expression of the PF markers elastin (*Eln*), fibulin-2 (*Fbln2*) and type XV collagen (*Col15a1*) was significantly enriched in Thy1 MCs (Figure 18A), whereas the HSC markers glial fibrillary acidic protein (*Gfap*) and lecithin-retinol acyltransferase (*Lrat*) were significantly expressed in HSCs (Figure 18B). Interestingly, cytoglobin (*Cygb*) and desmin (*Des*), which are conventional markers employed in immunohistochemistry

to define HSCs in liver sections, were expressed in both Thy1 MCs and HSCs. Additionally, the PF marker NTPDase2 (*Entpd2*) was significantly enriched in Thy1 MCs, and also in BECs (Figure 18A). The expression of NTPDase2 protein in BECs was evaluated by immunofluorescent staining, and co-localization with BEC marker CK19 was confirmed (Figure 20A). Next, expression changes of PFs markers in Thy1 MCs and HSCs collected from injured livers were also evaluated to validate specific enrichment of PFs (Figure 19). Although, expression levels of *Thy1* and *Fbln2* in Thy1 MCs and HSCs were maintained in normal and injured livers, interestingly, expression levels of *Eln* in HSCs increased in TAA injury and *Col15a1* increased in both DDC and TAA injury. Accordingly, elastin expression was observed in proximity to GFAP-expressing HSCs in TAA injured livers by immunostaining (Figure 20B). The apparent induction of elastin and type XV collagen in HSCs during liver injury suggests the ambiguity of the use of these molecules as PFs markers under certain conditions, as they may be expressed in both PFs and HSCs. Given that the known PF marker NTPDase2 was also expressed in biliary epithelial cells, Thy1 and fibulin-2 may stand as most reliable markers for PFs whose expression remains unchanged even in injured livers. Especially, Thy1 is a useful surface antigen marker for PFs due to its compatibility with selective isolation of live cells *in situ*. Taken together, it has been demonstrated that Thy1 MCs and HSCs are two distinct liver-resident mesenchymal cell populations, and it is suggested that Thy1 MCs are representative of the PF population.

Contribution of Thy1 MCs in pathogenesis of fibrosis upon liver injury

The observation above that Thy1 MCs and HSCs are two distinct myofibroblastic populations in the liver implicates their potential contribution to ECM synthesis upon liver injury. To determine specific roles of these cells *in vivo*, their nature in various mouse models of liver injury were examined. It has been suggested that the origin of hepatic myofibroblasts activated in response to chronic liver injury is dependent on the etiologies[20]. Besides, Thy1-expressing cells are reported to expand in response to progression of liver injury[25,26]. Accordingly, the expansion of Thy1-expressing cells in chronic liver injury models of different etiologies were examined; using, TAA administration and CCl_4 treatment as toxic liver injury models, and DDC-induced injury and common bile duct ligation (BDL) as cholestatic liver injury models (Figure 21A). Like TAA, CCl_4 is metabolized by zone 3 hepatocytes, giving rise to toxic trichloromethyl radicals, which mediate cytotoxic effects causing centri-lobular necrosis[38]. BDL causes a mechanical obstruction of the biliary tract[31], leading to peri-portal injury, like as DDC-induced liver injury. Immunodetection of Thy1 in liver sections of each chronic injury model revealed that Thy1 staining area expanded significantly upon DDC feeding and BDL, while TAA administration and CCl_4 injection resulted in little or no expansion (Figure 21B, 22A). Co-immunostaining of collagen type I and III in DDC injured liver revealed a massive accumulation of collagen in the peri-portal area, which resided in close proximity to expanding Thy1-expressing cells (Figure

23). Notably, Thy1-expressing cells co-localized with both types of collagen in normal uninjured liver as well. In contrast, accumulation of collagen in TAA injured liver was observed in the peri-central region and apart from Thy1-expressing cells. On the other hand, HSCs marked by GFAP, were located throughout the liver parenchyma, some of which resided near accumulated collagen in both DDC and TAA injured livers (Figure 24).

To further evaluate the contributions of Thy1 MCs and HSCs to the pathogenesis of fibrosis in liver injuries of different etiologies, comparative gene expression analysis was performed on specific liver cell populations freshly isolated from normal mouse livers and injured livers induced by DDC diet or TAA administration. Expression of collagens was enriched in Thy1 MCs and HSCs compared to other populations (Figure 25), indicating that these two populations are the main collagen producers in normal and injured livers. Interestingly, the expression level of collagen genes in Thy1 MCs and HSCs were comparable in DDC injured liver, while it was highly enriched in HSCs in TAA injured liver. In addition, HSCs showed marked increase in expression level of *Col1a1*, *Col3a1*, and *Acta2* in both injury models compared to normal (Figure 26), thus demonstrating their activation upon liver injury regardless of their etiologies. In contrast, Thy1 MCs did not show any change in expression level of either of the genes after 5 weeks of DDC administration, and rather showed the decrease of *Col1a1* and *Col3a1* upon TAA-induced liver injury (Figure 26).

Given the notion that portal fibroblasts may act as “first responders” in cholestatic liver injuries to produce collagen[39], the expression of *Col1a1 and Col3a1* were analyzed at 1 week of DDC-induced liver injury as well. Both Thy1 MCs and HSCs significantly increased the expression of these genes at this time point (Figure 26), thus promptly responding and contributing to fibrogenesis in the early phase of cholestatic liver injury, and then gradually waning thereafter. Notably, the expression level of tissue inhibitor of metalloproteinase 1(*Timp1*), an inhibitor of matrix metalloproteinase which degrades ECM, was increased in both Thy1 MCs and HSCs during DDC induced liver injury, while it was exclusively increased in HSCs during TAA induced liver injury (Figure 26). These results suggest that Thy1 MCs contribute to the pathogenesis of liver fibrosis by means of rapid fibrogenesis and inhibiting degradation of newly formed ECM, specifically during DDC-induced cholestatic liver injury.

The origin of expanding Thy1-expressing cells in cholestatic liver

While Thy1 MCs exclusively responded to and expanded upon cholestatic liver injury, it remains elusive as to whether these reactive Thy1 MCs are liver resident cells or of extra-hepatic origin. The expansion of Thy1-expressing cells in the time course of DDC-induced liver injury was followed, revealing that it increased significantly within the initial 1-2 weeks of feeding and seemed to saturate thereafter (Figure 22B). In order to assess whether resident Thy1-expressing cells

proliferated within this period, the thymidine analog EdU was administered in mice fed with DDC diet (Figure 27A). Immunostaining analysis of mouse liver sections revealed EdU incorporation in peri-portal Thy1-expressing cells, along with many other cells, such as BECs (Figure 27B). Meanwhile only a minor level of EdU incorporation was observed in normal livers under uninjured conditions (Figure 28A and 28B). This was further assessed by quantitative flow cytometric analysis, where a significantly higher proportion of Thy1 MCs incorporated EdU upon DDC-induced liver injury (Figure 28C). These results suggest that expansion of Thy1-expressing cells in cholestatic liver injury can be partly attributed to the proliferative reaction of resident cells.

It has been documented that bone marrow-derived fibrocytes infiltrate the liver upon chronic injury and convert into collagen-producing myofibroblasts[9], which led to the investigation of the possible involvement of bone marrow cells as an extra-hepatic origin of the expanded Thy1 MCs in our experimental settings. Whole bone marrow cells isolated from GFP-transgenic mice were transplanted to lethally irradiated wild type mice for bone marrow reconstitution. The bone marrow-reconstituted mice were subsequently fed with DDC diet, and analyzed for the presence of GFP^+ cells in chronically injured liver (Figure 29A). By immunofluorescent observation, massive infiltration of GFP^+ cells surrounding the portal vein in DDC-injured livers was detected, some of which apparently co-expressed Thy1 (Figure 29B). Flow cytometric analyses focusing on the $Thy1^+$

CD45$^-$ cell populations revealed that GFP$^+$ cells were rarely found in that population under uninjured conditions in bone marrow-reconstituted mice, whereas that there was a significant increase of GFP$^+$ cells therein upon DDC-induced injury (Figure 30). These results suggest that there are bone marrow-derived Thy1-expressing cells that are recruited into the liver upon DDC liver injury, which partly accounts for the increase and expansion of the peri-portal Thy1-expressing cells, in addition to proliferation of the resident cells.

To further characterize the nature of those bone marrow-derived cells, Thy1$^+$ CD45$^-$ cells were sorted based on the presence or absence of the GFP fluorescence and analyzed for the expression of representative characteristic genes of Thy1 MCs. Surprisingly, GFP$^+$ Thy1$^+$ CD45$^-$ cells did not express significant levels of *Fgf7, Col1a1, Col3a1 or Acta2* compared to GFP$^-$ Thy1$^+$ CD45$^-$ cells (Figure 31), indicating that bone marrow-derived Thy1-expressing cells do not contribute significantly to the fibrogenic reaction in cholestatic liver injury as collagen producing cells, despite their marked infiltration upon injury. On the other hand, expression of *Timp1* was comparable between GFP$^+$ cells and GFP$^-$ cells. Additionally, expression of PF markers was analyzed, which showed comparable expression of *Eln* between the two populations, whereas *Fbln2* was exclusively expressed in GFP$^-$ cells (Figure 32). These results suggest that proliferation and expansion of liver-resident Thy1$^+$ PFs make a predominant contribution to fibrogenic reaction in the peri-portal region upon cholestatic injury.

Discussion

The relation of Thy1-expressing cells to oval cells

In the liver pathobiology, Thy1 was first characterized in rat liver as a marker for oval cells[24] and they were shown to expand in conditions of stem/progenitor cell mediated hepatic regeneration. However, these histological analyses were solely performed in serial sections, which did not allow accurate evaluation of cell markers. In the present study, this notion was revisited using high-sensitive methods, such as confocal microscopy and flow cytometry, to evaluate the expression of typical oval cell markers in Thy1-expressing cells. By immunostaining and flow cytometic analysis, no co-expression of Thy1 and oval cell markers was observed in both normal and injured livers. Thus, these results indicate Thy1-expressing cells do not mark the typical stem cell population of chronically injured livers. Instead, later studies readdressed Thy1 as a marker for hepatic myofibroblasts, shown by co-localization with the myofibroblast marker α-SMA[28]. However, the functions of Thy1-expressing cells were not assessed in detail even in later studies, and Thy1 has rather been applied conveniently as a cell marker for "portal myofibroblasts" without precise confirmation, particularly in mouse studies.

Thy1 as a marker of liver-resident portal fibroblasts

In the present study, detailed characterization of Thy1-expressing cells in the mouse liver has shown that Thy1-expressing mesenchymal cells in chronically

injured liver in fact constitute a myofibroblast population and contribute to collagen synthesis. Thy1-expressing cells in the liver was a heterogeneous population, which consisted of T lymphocytes and mesenchymal cells that could be distinguished based on the presence or absence of the expression of the leukocyte marker CD45, showing distinct morphology and anatomic location in the liver tissue. Identification of Thy1-expressing mesenchymal cells by surface markers Thy1 and CD45 allowed the analysis of their characteristics in detail through *in vitro* analysis upon cell isolation and flow cytometry. As a result, Thy1-expressing mesenchymal cells were demonstrated to show characteristics of typical fibroblasts, and that of collagen producing myofibroblasts upon culture. This was particularly shown by the expression of α-SMA and collagen type I and III, at both transcriptional and protein levels. In addition to their myofibroblastic activation, these cells were enriched of expression of markers of PFs, such as *Eln*, *Fbln2*, *Col15a1*, and *Entpd2*. These results, together with their anatomical location around the portal vein, suggest that Thy1-expressing mesenchymal cells represent a major part, if not all, of PFs.

Characterization and distinction of Thy1 MCs and HSCs

Thy1 MCs and HSCs are distinct myofibroblast precursors, which can be distinguished by Thy1-expression and vitamin A-storing lipid autofluorescence, respectively, by flow cytometry. Until recently, identification of various cell types that constitute the liver largely depended on staining of specific markers by

immunohistochemical analysis. The present study allowed the isolation of mutually exclusive populations of Thy1 MCs and HSCs by flow cytometry-based analysis, followed by comparative gene expression analysis using quantitative RT-PCR. Interestingly, conventional markers used to identify HSCs, such as *Des* and *Cygb*, were also expressed in Thy1 MCs. Therefore, mesenchymal cells in the peri-portal region that express desmin may have been misinterpreted as HSCs in previous studies. In addition, the PF marker *Eln* and *Col15a1* expression was upregulated in HSCs by TAA liver injury, while expression of *Thy1* and *Fbln2* was unchanged. Immunostaining of elastin was confirmed around the portal vein which co-localized with peri-portal Thy1-expressing cells in normal and injured livers. Additionally, in TAA injured livers, elastin staining was also observed in the parenchyma, which resided in close proximity to GFAP-expressing cells. Elastin expression by HSCs in CCl_4-induced liver injury has been also reported[40], together indicating the induction of *Eln* expression in HSCs under certain conditions. Furthermore, expression of PF marker NTPDase2 was confirmed in BECs in addition to Thy1 MCs. Weak staining of NTPDase2 was observed in BECs marked by CK19, thus suggesting NTPDase2 expression alone does not necessarily define the PF population. These results suggest the ambiguity of cell type identification by the use of markers such as desmin, cytoglobin, elastin, and NTPDase2. Meanwhile, expression of fibulin-2 may be a strong marker for PFs. However, these available markers were not applicable for selective isolation of PFs. Instead, isolation of PFs has been achieved by outgrowth, size-selection methods,

and flow cytometry-based exclusion methods. None of these methods identify PFs by positive selection. Here, the combinatorial use of the surface antigens Thy1 and CD45 has allowed us, for the first time, to identify a mesenchymal population that presumably represents PFs by means of positive selection. Importantly, Thy1 expression and vitamin A autofluorescence was mutually exclusive, thus indicating that Thy1 MCs and conventional HSCs are two clearly distinct myofibroblast precursor populations.

Although Thy1 MCs and HSCs were undoubtedly distinct populations, they also shared common cell marker expression and fibrogenic properties in response to injury, suggesting their close lineage. Accordingly, it has been reported that PFs and HSCs share a common origin in the stage of liver development, where they are both derived from the mesothelium[41,42]. Although it is necessary to confirm that Thy1 MCs of the present study are derived from the mesothelium, due to their similar characteristics, it is reasonable that Thy1 MCs and HSCs may share an overlapping developmental origin.

Contribution of Thy1 MCs and HSCs to pathogenesis of liver fibrosis

Hepatic fibrosis is the most common outcome of many types of chronic liver diseases. While myofibroblasts play a critical role in the development of hepatic fibrosis, they are believed to originate from different cellular sources, depending on the etiologies. Using experimental liver injury models, it has been implicated that fibrogenic

myofibroblasts originate from HSCs in chronic toxic liver injuries, while on the other hand they originate from PFs in cholestatic liver injuries[20,43]. In mouse experimental models, chronic toxic liver injuries caused by CCl_4 or TAA administration result in hepatocellular necrosis around the central vein, whereas cholestatic liver injuries caused by DDC diet or BDL surgery result in injury of cholangiocytes in the portal region[44]. The anatomical location of HSCs, which are in the space of Disse, and PFs, in the portal mesenchyme, seems well compatible to the areas of injury and subsequent collagen accumulation in each experimental models. Nevertheless, the significance and the relative contribution of collagen synthesis and deposition by PFs compared to HSCs during liver injury remains largely controversial, in that reports on HSCs-specific genetic labeling using Lrat- or PDGFRβ-driven Cre transgenic mice have suggested that HSCs contribute mainly to the pathogenesis of hepatic fibrosis, regardless of the etiologies[45,46]. This controversy can be attributed at least in part to the lack of specific markers to identify PFs to compare them directly with HSCs with respect to their contribution in collagen synthesis and deposition, both quantitatively and qualitatively. Rather, previous studies identified them by negative selection, specifically, the lack of vitamin A autofluorescence[16] or of genetically labeled HSC markers[45,46]. Based upon the notion that Thy1-expressing mesenchymal cells represent PFs, the present study have clearly demonstrated that PFs react exclusively in models of cholestatic liver injury and contribute to collagen synthesis in addition to conventional HSCs.

The present study showed that expression of fibrogenic genes in Thy1 MCs was relatively high even in normal livers compared to other cell populations, along with noticeable deposition of collagen fibers around the portal vein. These results indicate that Thy1 MCs produce collagen fibers in physiological conditions even without fibrous stimuli of injured liver, presumably to maintain the structure of the portal triad and contributing to the turnover of ECM in the Glisson's capsule. In mouse models of cholestatic liver injury, ECM accumulation is observed in the peri-portal region along with the expansion of Thy1-expressing cells. Surprisingly, expression of *Col1a1*, *Col3a1* and *Acta2* did not change significantly in Thy1 MCs between normal and DDC injured mice at 5 weeks. Although, as "first responders" of cholestatic liver injury, Thy1 MCs increased expression of *Col1a1* and *Col3a1* about 3 fold compared to normal, at 1 week of DDC induced liver injury, expression of *Timp1* was induced even more drastically (about 20 fold compared to normal). This indicated that qualitative changes in Thy1 MCs accompanied predominant "suppression of fibrolysis" rather than "fibrogenesis" during cholestatic liver injury, especially at an early time point, thus contributing to the accumulation of ECM in the peri-portal area. On the other hand, HSCs contribute to the pathogenesis of liver fibrosis by means of increasing production (fibrogenesis) and inhibiting degradation (fibrolysis) of ECM simultaneously, in both DDC and TAA induced liver injury. Especially, HSCs were major contributors of the pathogenesis of liver fibrosis over Thy1-expressing cells in models of toxic liver injury, consistent with

previous references[47,48]. Therefore, Thy1 MCs contribute specifically to pathogenesis of liver fibrosis in models of cholestatic liver injury, whereas HSCs contribute to liver fibrosis in models of both cholestatic and toxic liver injury.

The mode of reaction by Thy1-expressing cells upon cholestatic liver injury

Thy1-expressing cells specifically react to cholestatic liver injury, shown by their expansion in injured liver sections. It has been suggested from the present study, that liver-resident Thy1-expressing cells rapidly proliferate in response to the onset of DDC-induced cholestatic injury. The factors that may induce this rapid response in Thy1-expressing cells are of special interest for the development of a therapeutic strategy. Platelet-derived growth factor is the most potent mitogen for HSCs *in vitro* and *in vivo*[49]. However, the receptors PDGFRα and β expression are both absent in Thy1 MCs of normal liver. Thus, it is suggested that other factors may be involved in the proliferation of Thy1 MCs during cholestatic liver injury. The mechanisms of PFs activation *in vivo* upon liver injury are of special future interest.

Bone marrow-derived fibrocytes have been suggested to infiltrate upon liver injury, although their specific contribution to the pathogenesis of liver fibrosis is controversial[50,51]. In the current study, it has been elucidated that a significant portion of Thy1-expressing mesenchymal cells are derived from the bone marrow

upon cholestatic liver injury. These bone marrow-derived cells expressed fibrogenic genes, although significantly lower compared to liver-resident Thy1-expressing mesenchymal cells. Interestingly, expression of *Eln* and *Timp1* was comparable between the two populations, thus suggesting that these bone marrow-derived cells account to a portion of PFs, and may contribute to fibrotic response upon liver injury at least in part through suppression of fibrolysis. On the other hand, the lack of *Fbln2* expression clearly distinguished the bone marrow-derived cells from liver-resident PFs. The exact identity and function of the former cells are yet to be determined, especially in view of their relationship to fibrocytes. Fibrocytes are defined as $CD45^+$ collagen-expressing cells derived from the bone marrow[52], whereas the population of interest in the current study is $CD45^-$. The possibility that fibrocytes lose CD45 expression after infiltration into injured livers cannot be omitted, which was not assessed in the current study due to the lack of appropriate tools for lineage tracing. Further characterization on this unique cell population is of significant interest and should be done in future studies.

Conclusion

In conclusion, it has been demonstrated that the surface antigen Thy1 stands as an effective and reliable marker to identify and isolate a representative population, if not all, of PFs. Traditionally, cell populations that constitute the liver has been identified and defined mainly by their morphology and anatomical location. Through the years, rigorous efforts on identification of cell specific markers, especially of surface antigens, have enabled prospective isolation and an in-depth analysis of liver cell populations, such as EpCAM for BECs[17], Stab-2 for LSECs[18] and so forth. Nevertheless, PFs still lacked a specific cell surface antigen for selective isolation. Although Thy1 has been suggested, precise confirmation has not been empirically accomplished. The analysis of Thy1-expressing cells that presumably represent PFs uncovered the under-estimated role of these cells as an augmentative contributor in ECM accumulation, in addition to conventional HSCs, during the pathogenesis of liver fibrosis in cholestatic liver injury. Whereas HSCs have been generally considered as the major contributor of ECM accumulation in fibrotic livers and thus have been the center of attention as a therapeutic target[53], the present study suggests that the cell types involved in the pathogenesis of liver fibrosis should vary according to its etiology. Thus, careful diagnosis to assess the pathology of liver fibrosis is required for effective targeting and prospective treatment.

References

1. Kmiec Z. Cooperation of liver cells in health and disease. Adv Anat Embryol Cell Biol. 2001; 161:III-XIII, 1-151.

2. Gebhardt R. Metabolic zonation of the liver: regulation and implications for liver function. Pharmacol Ther. 1992;53(3):275-354.

3. Arthur MJ. Fibrogenesis II. Metalloproteinases and their inhibitors in liver fibrosis. Am J Physiol Gastrointest Liver Physiol. 2000; 279(2): G245-9.

4. Friedman SL, Roll FJ, Boyles J, Bissell DM. Hepatic lipocytes: the principal collagen-producing cells of normal rat liver. Proc Natl Acad USA 1989; 82(24): 8681-5.

5. Senoo H, Kojima N, Sato M. Vitamin A-storing cells (stellate cells). Vitam Horm 2000; 75: 131-59.

6. Troeger JS, Mederacke I, Gwak GY, Dapito DH, et al. Deactivation of hepatic stellate cells during liver fibrosis resolution in mice. Gastroenterology 2012; 143(4): 1073-83.

7. Seki E, Brenner DA. Recent advancement of molecular mechanisms of liver fibrosis. J Hepatobiliary Pancreat Sci 2015; 22(7): 512-8.

8. Kinnman N, Francoz C, Barbu V, Wendum D, Rey C, et al. The myofibroblastic conversion of peribiliary fibrogenic cells distinct from hepatic stellate cells is stimulated by platelet-derived growth factor during liver fibrogenesis. Lab Invest 2003; 83(2): 163-73.

9. Kisseleva T, Uchinami H, Feirt N, Quintana-Bustamante O, et al. Bone marrow-derived fibrocytes participate in pathogenesis of liver fibrosis. J Hepatol 2006; 45(3): 429-38.

10. Li Y, Wang J, Asahina K. Mesothelial cells give rise to hepatic stellate cells and myofibroblasts via mesothelial-mesenchymal transition in liver injury. Pro Natl Acad Sci USA 2013; 110(6): 2324-9.

11. Beaussier M, Wendum D, Schiffer E, Dumon S, et al. Prominent contribution of portal mesenchymal cells to liver fibrosis in ischemic and obstructive cholestatic injuries. Lab Invest 2007; 87(3): 292-303.

12. Dranoff JA, Wells RG. Portal fibroblasts: Underappreciated mediator of biliary fibrosis. Hepatology 2010; 51(4): 1438-44.

13. Wells RG. The portal fibroblast: not just a poor man's stellate cell. Gastroenterology 2014; 147(1): 41-7.

14. Uchio K, Tuchweber B, Manabe N, Gabbiani G, Rosenbaum J, et al. Cellular retinol-binding protein-1 expression and modulation during in vivo and in vitro myofibroblastic differentiation of rat hepatic stellate cells and portal fibroblasts. Lab invest 2002; 82(5): 619-28.

15. Wen JW, Olsen AL, Perepelyuk M, Wells RG. Isolation of rat portal fibroblasts by in situ liver perfusion. J Vis Exp 2012; (64): pii:3669.

16. Iwaisako K, Taura K, Koyama Y, Takemoto K, et al. Strategies to detect hepatic myofibroblasts in liver cirrhosis of different etiologies. Curr Pathobiol Rep 2014; 2(4): 209–215.

17. Okabe M, Tsukahara Y, Tanaka M, Suzuki K, et al. Potential hepatic stem cells reside in EpCAM+ cells of normal and injured mouse liver. Development 2009; 136(11): 1951-60.

18. Nonaka H, Sugano S, Miyajima A. Serial analysis of gene expression in sinusoidal endothelial cells from normal and injured mouse liver. Biochem Biophys Res Commun 2004; 324(1): 15-24.

19. Onitsuka I, Tanaka M, Miyajima A. Characterization and functional analysis of hepatic mesothelial cells in mouse liver development. Gastroenterology 2010; 138(4): 1525-35.

20. Iwaisako K, Jian C, Zhang M, Cong M, et al. Origin of myofibroblasts in the fibrotic liver in mice. Proc Natl Acad Sci USA 2014; 111(32): E3297-305.

21. Lua I, Li Y, Zagory JA, Wang KS, et al. Characterization of hepatic stellate cells, portal fibroblasts, and mesothelial cells in normal and fibrotic livers. J Hepatol 2016; 64(5): 1137-46.

22. Miyajima A, Tanaka M, Itoh T. Stem/progenitor cells in liver development, homeostasis, regeneration, and reprogramming. Cell Stem Cell 2014; 14(5): 561-74.

23. Grompe M. Liver stem cells, where art thou? Cell Stem Cell 2014; 15(3): 257-8.

24. Petersen BE, Goff JP, Greenberger JS, Michalopoulos GK. Hepatic oval cells express the hematopoietic stem cell marker Thy-1 in the rat. Hepatology 1998; 27(2): 433-45.

25. Takase HM, Itoh T, Ino S, Wang T, et al. FGF7 is a functional niche signal required for stimulation of adult liver progenitor cells that support liver regeneration. Genes Dev 2013; 27(2): 169-81.

26. Yovchev MI, Zhang J, Neufeld DS, Grozdanov PN, et al. Thymus cell antigen-1-expressing cells in the oval cell compartment. Hepatology 2009; 50(2): 601-11.

27. Liu D, Yovchev MI, Zhang J, Alfleri AA, et al. Identification and characterization of mesenchymal-epithelial progenitor-like cells in normal and injured rat liver. Am J Pathol 2015; 185(1): 110-28.

28. Dudas J, Mansuroglu T, Batusic D, Saile B, et al. Thy-1 is an in vivo and in vitro marker of liver myofibroblasts. Cell Tissue Res 2007; 329(3): 503-14.

29. Dezso K, Jelnes P, Laszlo V, Baghy K, et al. Thy-1 is expressed in hepatic myofibroblasts and not oval cells in stem cell-mediated liver regeneration. Am J Pathol 2007; 171(5): 1529-37.

30. Dudas J, Mansuroglu T, Batusic D, Ramadori G. Thy-1 is expressed in myofibroblasts but not found in hepatic stellate cells following liver injury. Histochem Cell Biol 2009; 131:115-127.

31. Tag CG, Sauer-Lehnen S, Weiskirchen S, Borkham-Kamphorst E, et al. Bile duct ligation in mice: induction of inflammatory liver injury and fibrosis by obstructive cholestasis. J Vis Exp 2015; Feb 10;(96).

32. Cole SP, Marks GS. Ferrochelatase and N-alkylated porphyrins. Mol Cell Biochem 1984; 64(2): 127-37.

33. Fickert P, Stoger U, Fuchsbichler A, Moustafa T, et al. A new xenobiotic-induced mouse model of sclerosing cholangitis and biliary fibrosis. Am J Pathol 2007; 171(2): 525-36.

34. Hajovsky H, Hu G, Koen Y, Sarma D, et al. Metabolism and toxicity of thioacetamide S-oxide in rat hepatocytes. Chem Res Toxicol 2012; 25:1955–63.

35. Wells RG, Schwabe RF. Origin and function of myofibroblasts in the liver. Semin Liver Dis 2015; 35(2): 97-106.

36. Mederacke I, Dapito DH, Affo S, Uchinami H, et al. High-yield and high-purity isolation of hepatic stellate cells from normal and fibrotic mouse livers. Nat Protoc 2015; 10(2): 305-15.

37. De Minicis S, Seki E, Uchinami H, Kluwe J, et al. Gene expression profiles during hepatic stellate cell activation in culture and in vivo. Gastroenterology 2007; 132(5): 1937-46.

38. Slater TF, Cheeseman KH, Ingold KU. Carbon tetrachloride toxicity as a model for studying free-radical mediated liver injury. Philos Trans R Soc Lond B Biol Sci 1985; 311:633–645.

39. Kinnman N, Housset C. Peribiliary myofibroblasts in biliary type liver fibrosis. Front Biosci 2002; 7: d496-503.

40. Kanta J, Dooley S, Delvoux B, Breuer S, et al. Tropoelastin expression is up-regulated during activation of hepatic stellate cells and in the livers of CCl_4--cirrhotic rats. Liver 2002 22(3):220-7.

41. Asahina K, Tsai SY, Li P, Ishii M, et al. Mesenchymal origin of hepatic stellate cells, submesothelial cells, perivascular mesenchymal cells during mouse liver development. Hepatology 2009; 49(3): 998-1011.

42. Lua I, James D, Wang J, Wang KS, et al. Mesodermal mesenchymal cells give rise to myofibroblasts, but not epithelial cells, in mouse liver injury. Hepatology 2014; 60(1): 311-22.

43. Battaler R, Brenner DA. Liver fibrosis. J Clin Invest 2005; 115(2): 209-18.

44. Liedtke C, Luedde T, Sauerbruch T, Scholten D, et al. Experimental liver fibrosis research: update on animal models, legal issues and translational aspects. Fibrogenesis Tissue Repair 2013; 6(1): 19.

45. Mederacke I, Hsu CC, Troeger Js, Huebener P, et al. Fate tracing reveals stellate cells as dominant contributors to liver fibrosis independent of its aetiology. Nat Commun 2013; 4: 2823.

46. Henderson NC, Arnold TD, Katamura Y, Giacomini MM, et al. Targeting of av integrin identifies a core molecular pathway that regulates fibrosis in several organs. Nat Med 2013; 19(12): 1617-24.

47. Tennakoon AH, Izawa T, Wijesundera KK, Murakami H, et al. Immunohistochemical characterization of glial fibrillary acidic protein (GFAP)-expressing cells in a rat liver cirrhosis model induced by repeated injections of thioacetamide (TAA). Exp Toxicol Pathol 2015; 67(1): 53-63.

48. Friedman SL. Evolving challenges in hepatic fibrosis. Nat Rev Gastroenterol Hepatol 2010; 7(8): 425-36.

49. Bonner JC. Regulation of PDGF and its receptors in fibrotic diseases. Cytokine Growth Factor Rev 2004; 15(4): 255-73.

50. Forbes SJ, Russo FP, Rey V, Burra P, et al. A significant portion of myofibroblasts are of bone marrow origin in human liver fibrosis. Gastroenterology 2004; 126(4): 955-63.

51. Higashiyama R, Moro T, Nakao S, Mikami K, et al. Negligible contribution of bone-marrow derived cells to collagen production during hepatic fibrogenesis in mice. Gastroenterology 2009; 137(4): 1459-66.

52. Abe R, Donnelly SC, Peng T, Bucala R, et al. Peripheral blood fibrocytes: differentiation pathway and migration to wound sites. J Immunol 2001;

166(2):7556–62.

53. Wu J, Zern MA. Hepatic stellate cells: a target for the treatment of liver fibrosis. J Gastroenterol 2000; 35(9): 665-72.

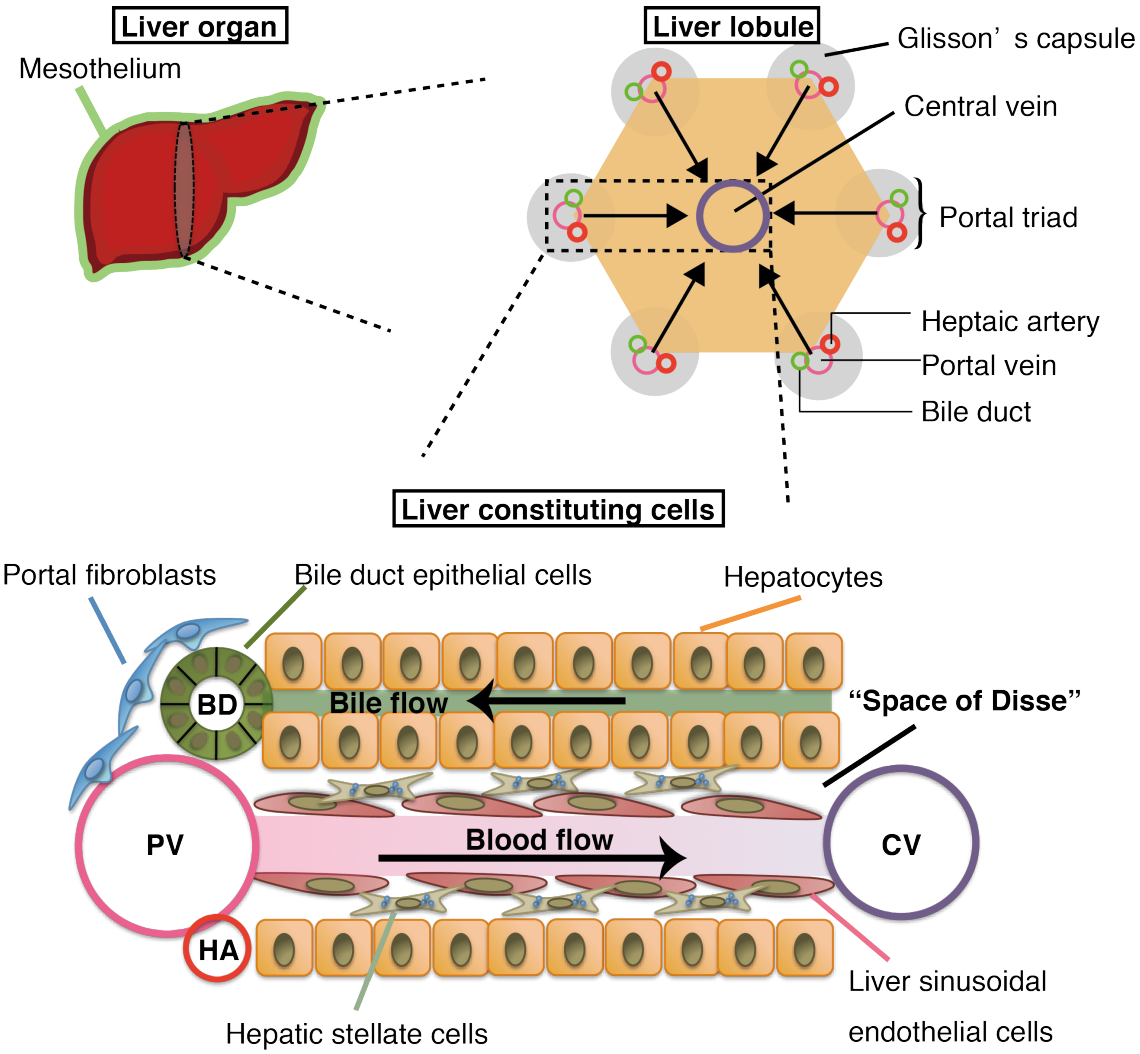

Figure 1. Liver structure and constituting cell types

The liver organ is encapsulated by the mesothelium. Liver lobule, which is the functional unit of the liver, is depicted. Portal triads, which consist of the portal vein, bile duct, and hepatic artery, surround the central vein, and blood flows from the portal vein and hepatic artery to the central vein. Liver constituting cells are depicted. Abbreviations: BD, bile duct; CV, central vein; HA, hepatic artery; PV, portal vein.

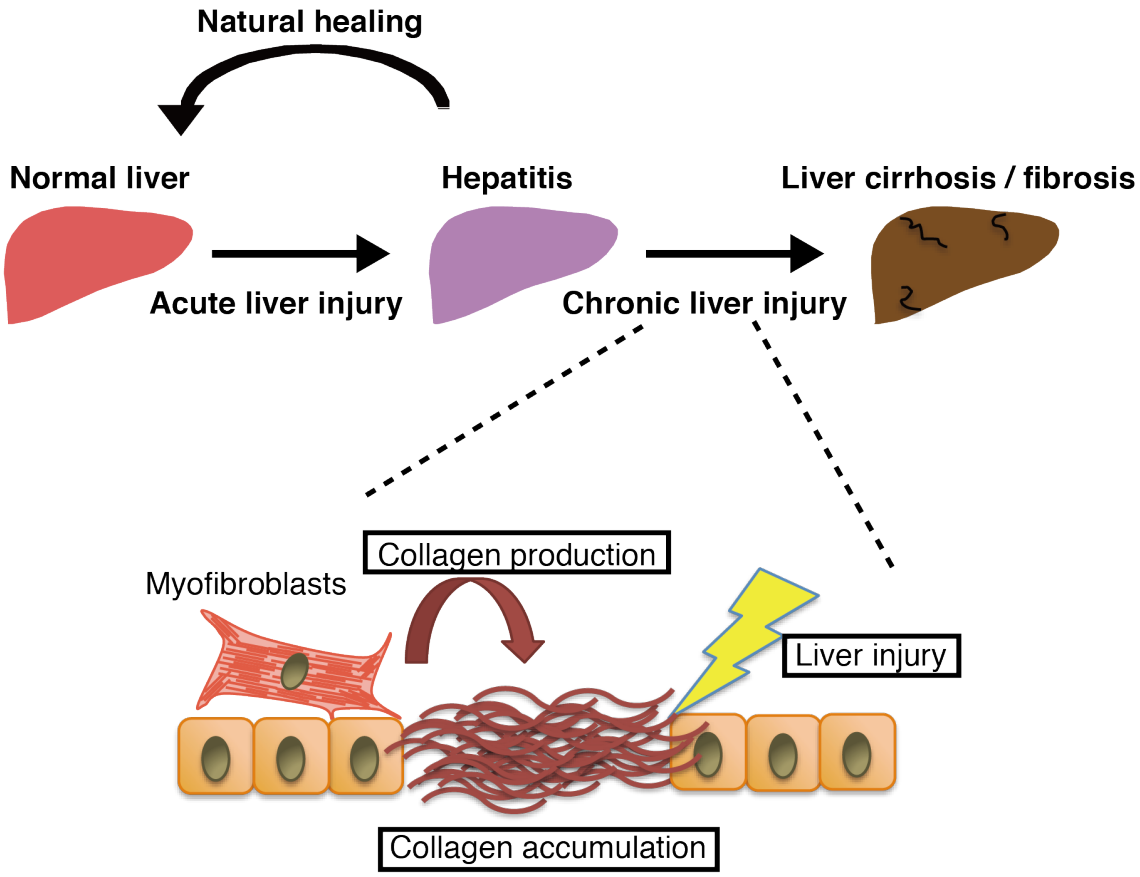

Figure 2. Liver cirrhosis/fibrosis is caused by chronic liver injury

Diagram of the processes that lead to liver cirrhosis, or fibrosis. Inflammation is caused in acute liver injury. If the damage subsides, the liver renders back into its normal state by means of natural healing. However, in cases of chronic liver injury, where there is continuous liver damage, there is excessive production and decreased degradation of ECM, including collagen, resulting in accumulation of collagen. This eventually leads to conditions such as liver cirrhosis or liver fibrosis.

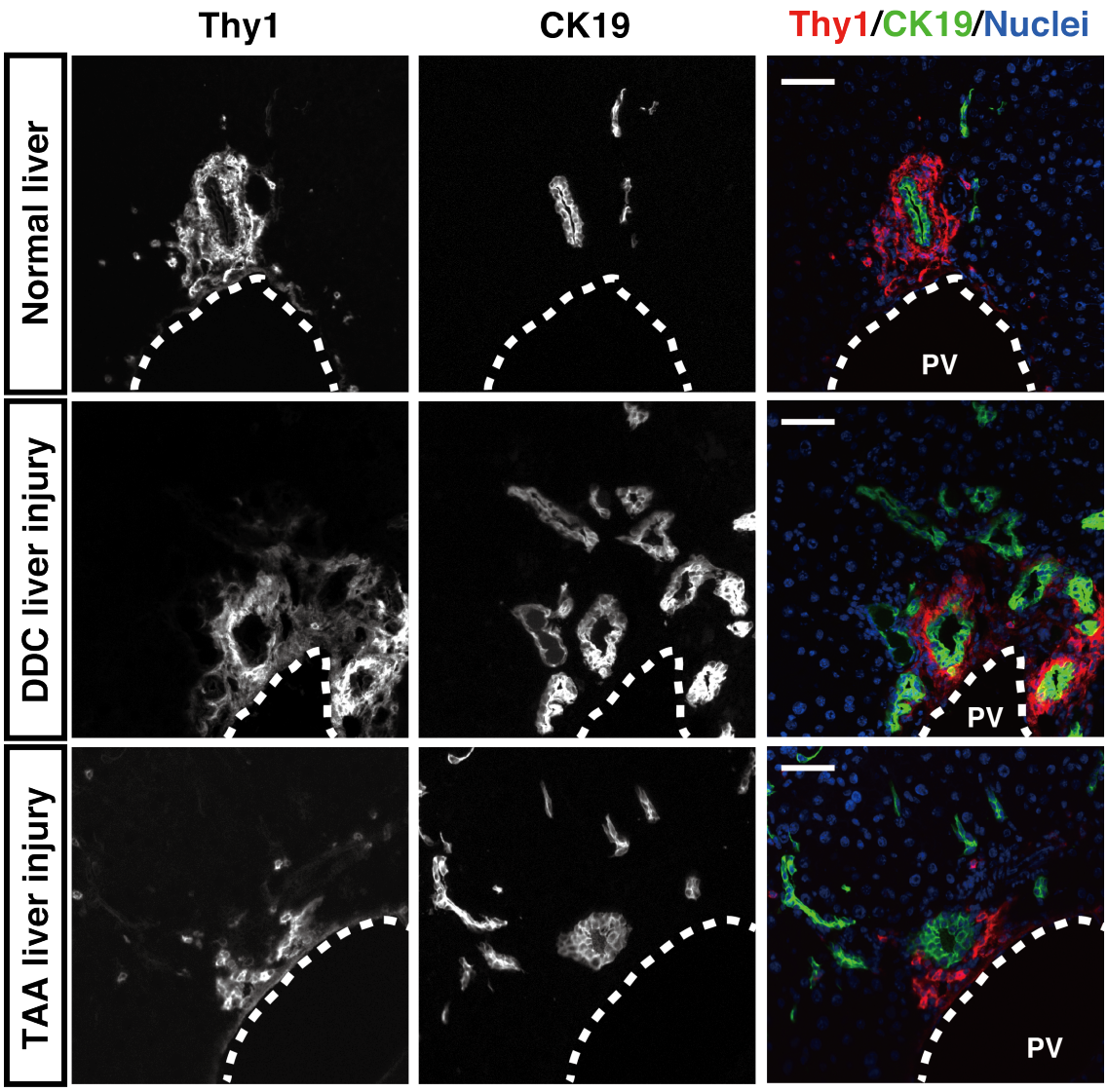

Figure 3. Relation of Thy1-expressing cells to oval cells in normal and chronically injured livers

Immunofluorescent staining of Thy1 (red) and CK19 (green) in liver tissue sections. Single staining is shown in gray scale, while merged image is shown with color. Nuclei were counterstained with Hoechst 33342 (blue). PV is traced with white dotted lines. Thy1-expressing cells in the portal region reside in proximity to CK19-expressing cells in normal and injured livers. Scale bars = 50 μm. Abbreviation: PV, portal vein.

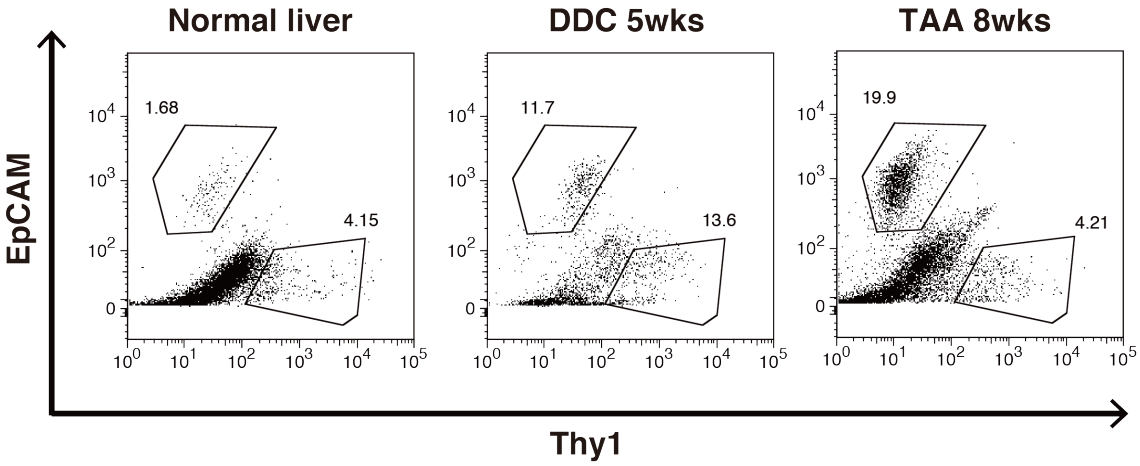

Figure 4. Flow cytometry of Thy1-expressing cells and oval cells in normal and chronically injured livers

Flow cytometric analysis of NPCs isolated from normal, DDC, and TAA livers. NPCs were stained with EpCAM and Thy1, and positive cells were sorted by MACS for purification. Thy1-expressing cells and EpCAM-expressing cells, which conventionally identify biliary epithelial cells and oval cells, are mutually exclusive populations in normal and injured livers. Dot plots shown are gated for PI^- and $CD45^-$. Representative dot plot is shown.

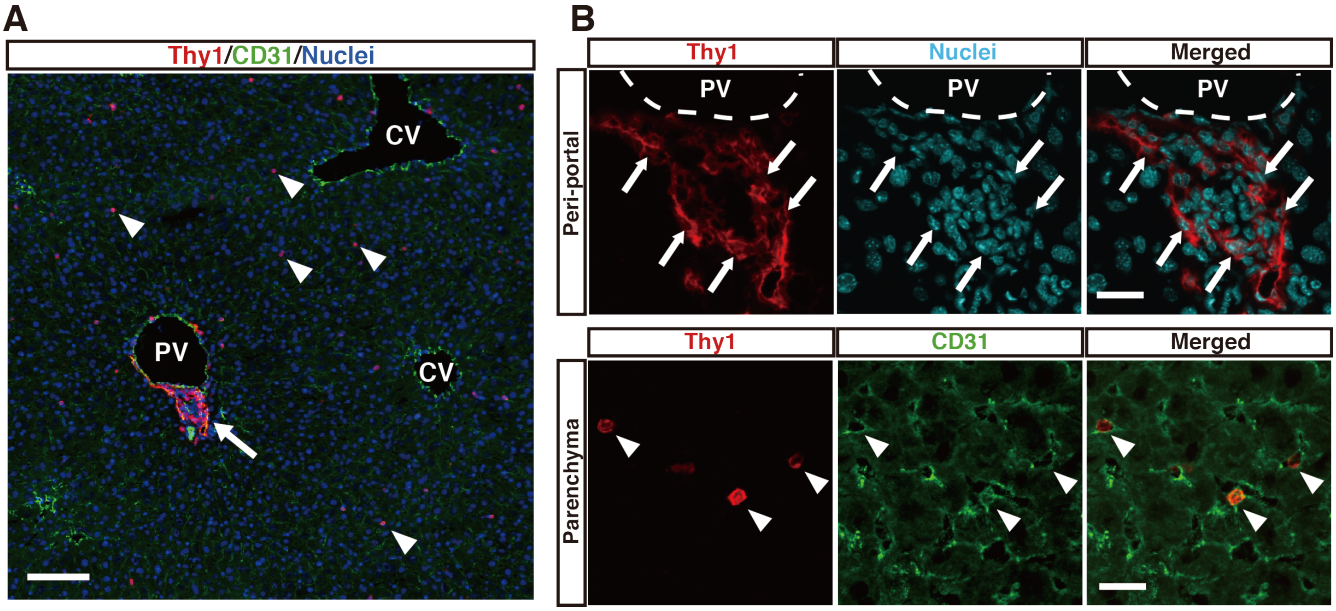

Figure 5. Immunostaining of two morphologically distinct Thy1-expressing cells in mouse liver tissue

(A) Immunofluorescent staining of Thy1 (red) and CD31 (green) in normal mouse liver section, demonstrating the anatomical distribution of two morphologically distinct Thy1-expressing cells. Arrow indicates Thy1-expressing cells residing near the portal vein. Arrowheads indicate Thy1-expressing cells distributed across the liver parenchyma. PV and CV are as indicated. Nuclei (blue) were counterstained with Hoechst 33342. Scale bar = 100 μm. (B) Magnified images of Thy1-expressing cells in different locations. Thy1 (red) and nuclei (cyan) staining are shown in upper panels. Arrow indicates planular and elongated Thy1-expressing cells. Thy1 (red) and CD31 (green) staining are shown in lower panels. Arrowheads indicate round and spherical Thy1-expressing cells existing within the luminal side of the sinusoid. Scale bars = 20 μm. PV is traced with white dotted lines. Abbreviations: CV, central vein; PV, portal vein.

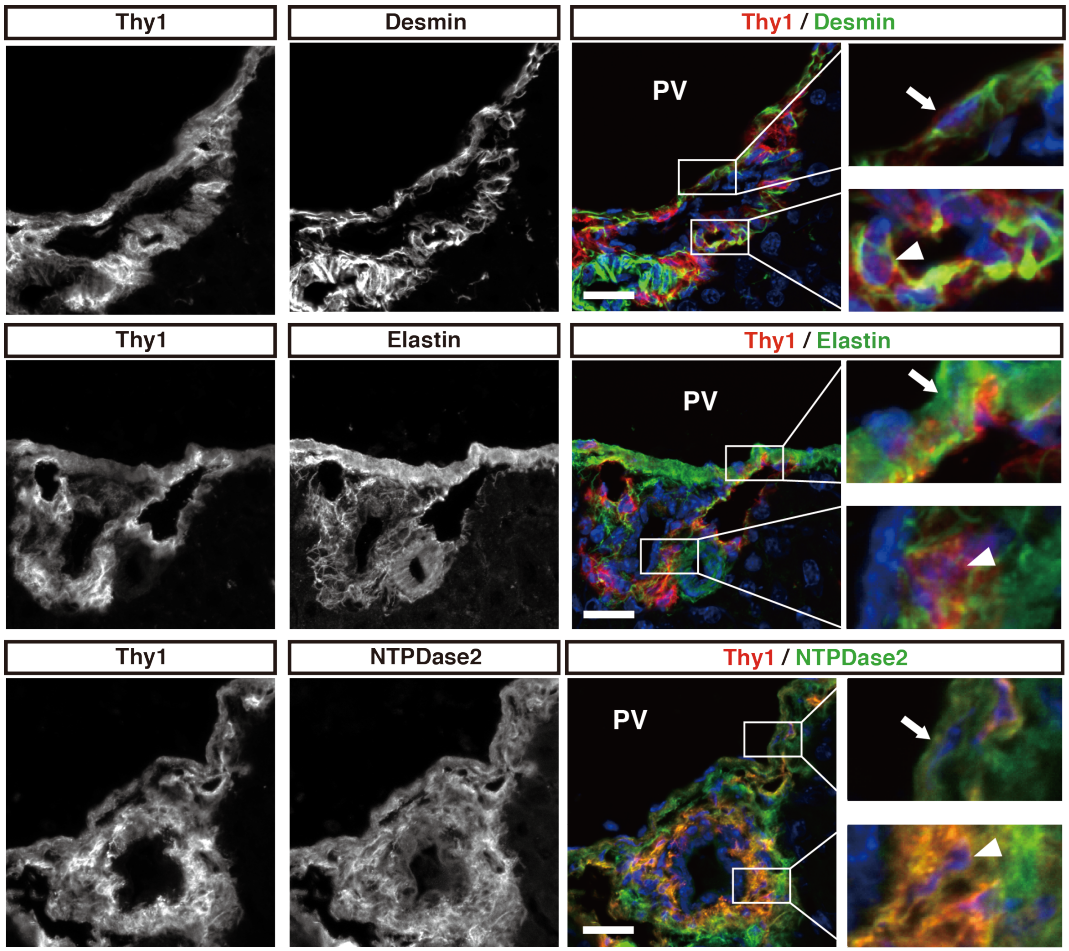

Figure 6. Expression of PFs markers in Thy1-expressing cells of normal liver sections

Immunostaining of Thy1 (red) and each mesenchymal and portal fibroblast markers (green) in normal mouse liver. Single staining images are shown in gray scale. Areas surrounded by white boxes are enlarged to the right. Arrows indicate expression in vascular walls of the portal vein. Arrowheads indicate co-expression of each marker with Thy1. Nuclei (blue) were counterstained with Hoechst 33342. Scale bars = 20 μm. Abbreviation: PV, portal vein.

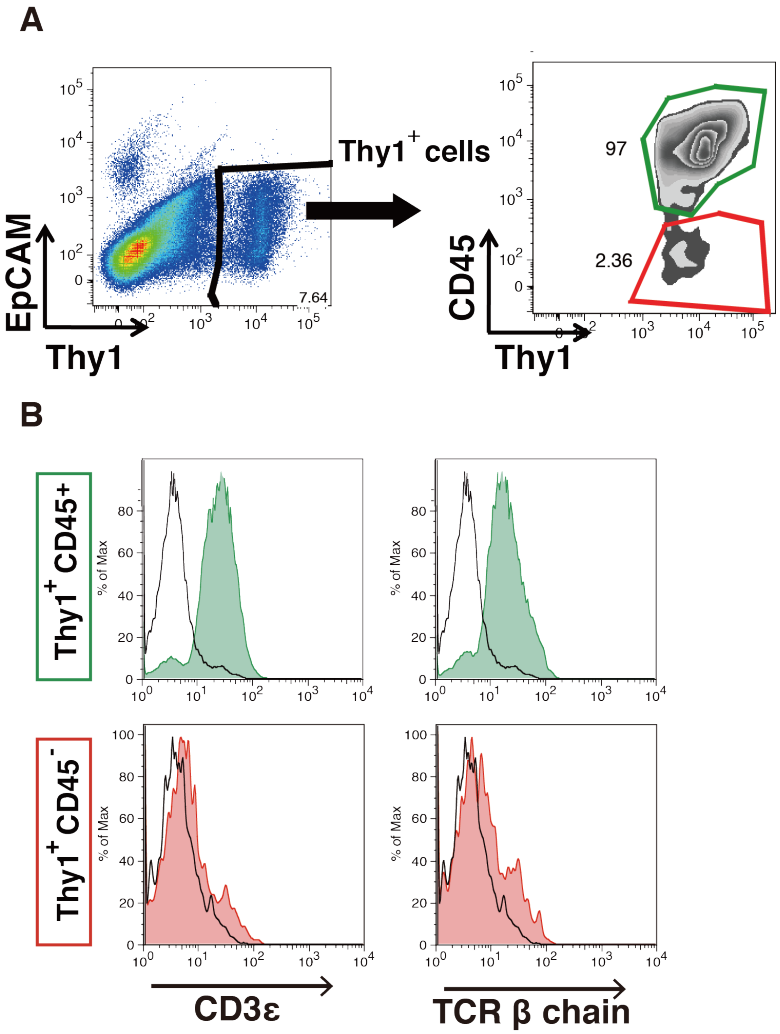

Figure 7. Subdividing Thy1-expressing cells based on the expression of leukocyte marker CD45

(A) Flow cytometric analysis of NPCs isolated from normal mouse liver. Thy1-expressing cells were gated out, which could be subsequently divided into two distinct subpopulations of $CD45^+$ $Thy1^+$ cells (green gate) and $CD45^-$ $Thy1^+$ cells (red gate). Representative dot plot is shown. (B) $CD45^+$ $Thy1^+$ cells and $CD45^-$ $Thy1^+$ cells were further characterized by the expression of T-cell markers by histogram plots. Green shaded lines indicate $CD45^+$ $Thy1^+$ cells and red shaded lines indicate $CD45^-$ $Thy1^+$ cells. Black lines indicate isotype control of the corresponding cell types. $CD45^+$ $Thy1^+$ cells expressed representative markers of T-cells.

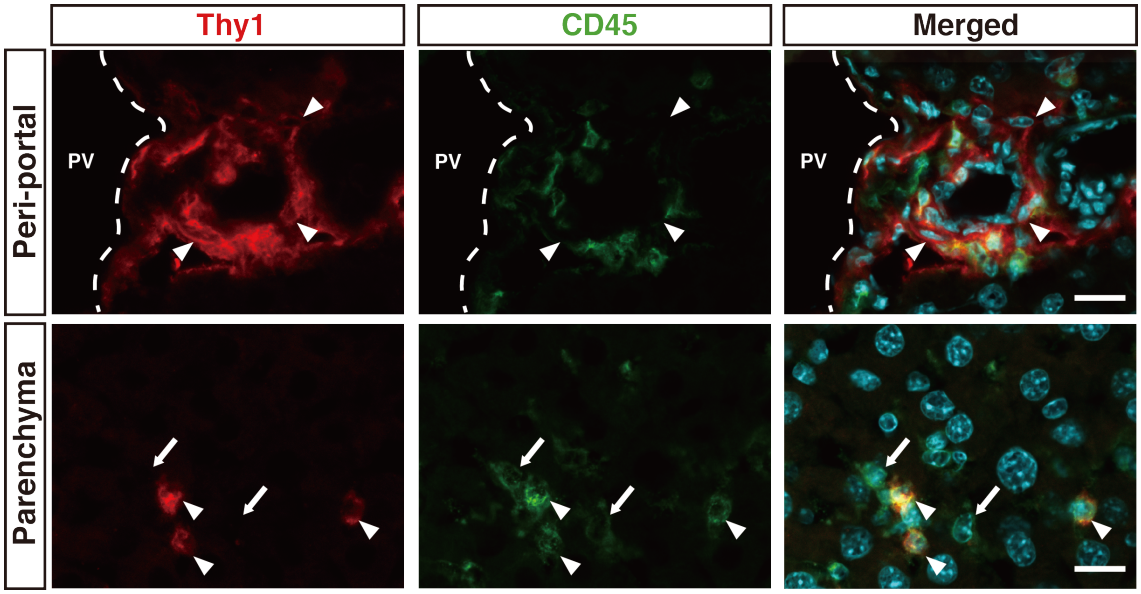

Figure 8. Immunostaining of Thy1-expressing cells with leukocyte marker CD45 in mouse liver tissue

Immunofluorescent staining of Thy1 (red) and CD45 (green) in normal mouse liver section, with upper panels showing the peri-portal region and lower panels showing the parenchymal region. Arrowheads in top panels indicate $CD45^-$ peri-portal Thy1-expressing cells. Arrows and arrowheads in lower panels indicate $Thy1^-$ $CD45^+$ cells and $Thy1^+$ $CD45^+$ cells, respectively. $CD45^-$ Thy1-expressing cells resided exclusively in the peri-portal area, whereas Thy1-expressing cells in the parenchyma was mostly $CD45^+$. Nuclei (cyan) were counterstained with Hoechst 33342. Scale bar = 20 μm. PV is traced with white dotted lines. Abbreviation: PV, portal vein.

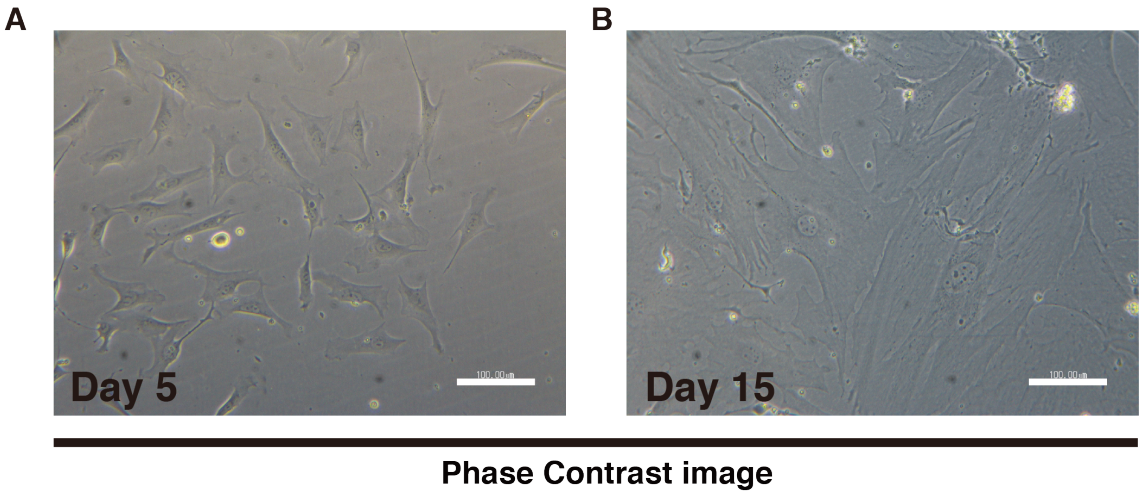

Figure 9. *In vitro* cultured Thy1-expressing cells show myofibroblastic morphology

(A, B) Phase contrast images of cultured Thy1-expressing cells, 5 days (A) or 15 days (B) after initial seeding. Thy1-expressing cells express fibroblastic morphology at Day 5, and gradually express morphology of myofibroblasts, shown by appearance of filamentous structures. Scale bars = 100 μm.

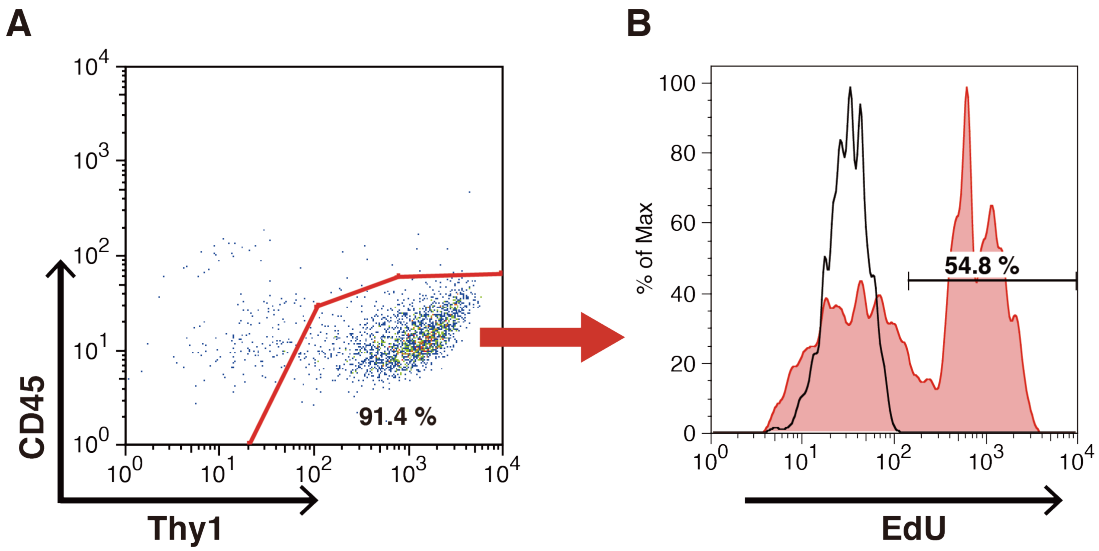

Figure 10. Purity of cultured Thy1-expressing cells and proliferation
(A) Flow cytometric analysis of cultured Thy1-expressing cells after 5 days of initial seeding. Cultured Thy1-expressing cells were mostly $CD45^-$ $Thy1^+$. (B) Flow cytometric analysis of EdU incorporation by Thy1-expressing cells shown by histogram plotting. After 5 days of initial seeding, EdU (5 μM) was added to the medium. Cells were analyzed 72 hours after the addition of EdU. Incorporation of EdU by $Thy1^+$ $CD45^-$ cells was determined in cells as gated in (A). Red shaded lines indicate $Thy1^+$ $CD45^-$ cells, and black lines indicate control experiment, where PBS was added to culture media. Cultured Thy1-expressing cells were proliferative. Histogram is representative of three independent experiments.

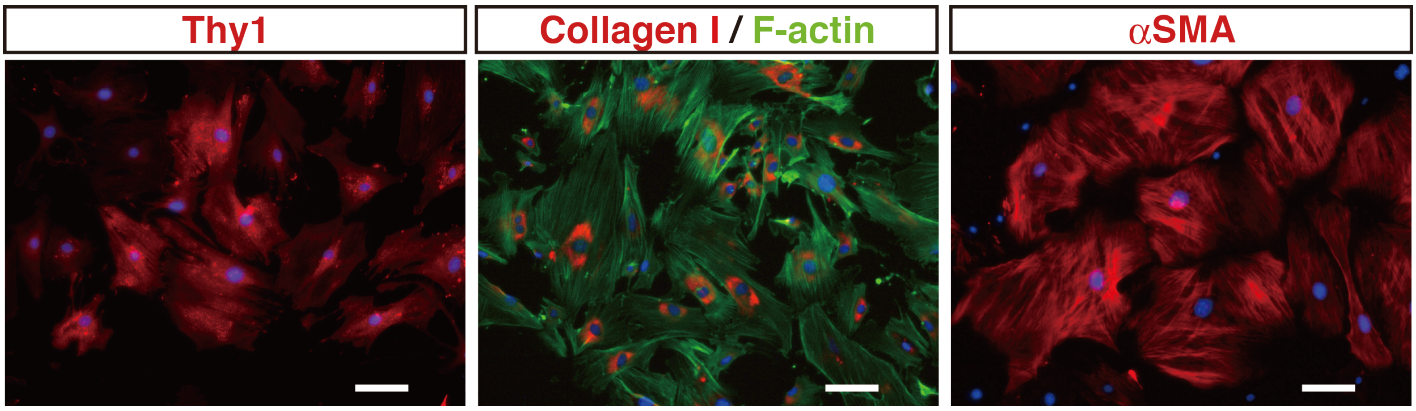

Figure 11. Expression of myofibroblast markers in cultured Thy1-expressing cells

Immunostaining for Thy1 (red in the left panel), collagen type I (red in the middle panel) , and α-SMA (red in the right panel) of Thy1-expressing cells cultured for 15 days. F-actin staining by phalloidin (green in the middle panel) is shown to confirm cell size. Cultured Thy1-expressing cells express markers of myofibroblasts, shown by their expression of Collagen I and αSMA. Scale bars = 100 μm.

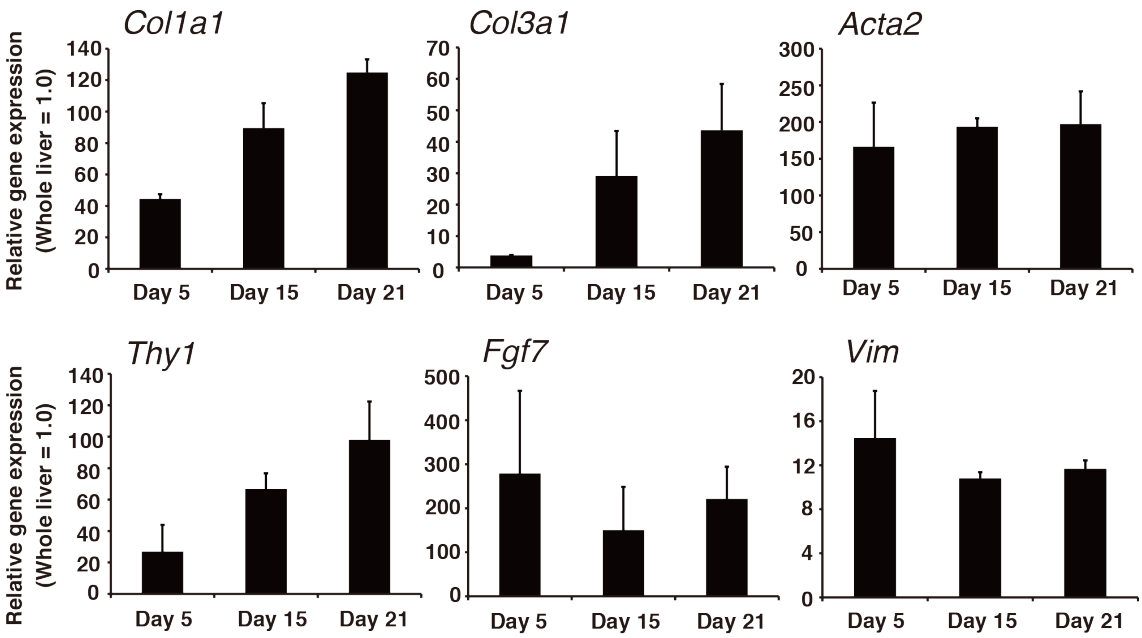

Figure 12. Gene expression analysis of (myo)fibroblast markers in cultured Thy1-expressing cells

Gene expression analysis by quantitative RT-PCR analysis of cultured Thy1-expressing cells at the indicated time points. Expression level of each gene is shown relative to the expression level of normal whole liver sample as 1.0. All gene expression was normalized with β-actin expression. n = 3 for each group. Error bars represent SEM.

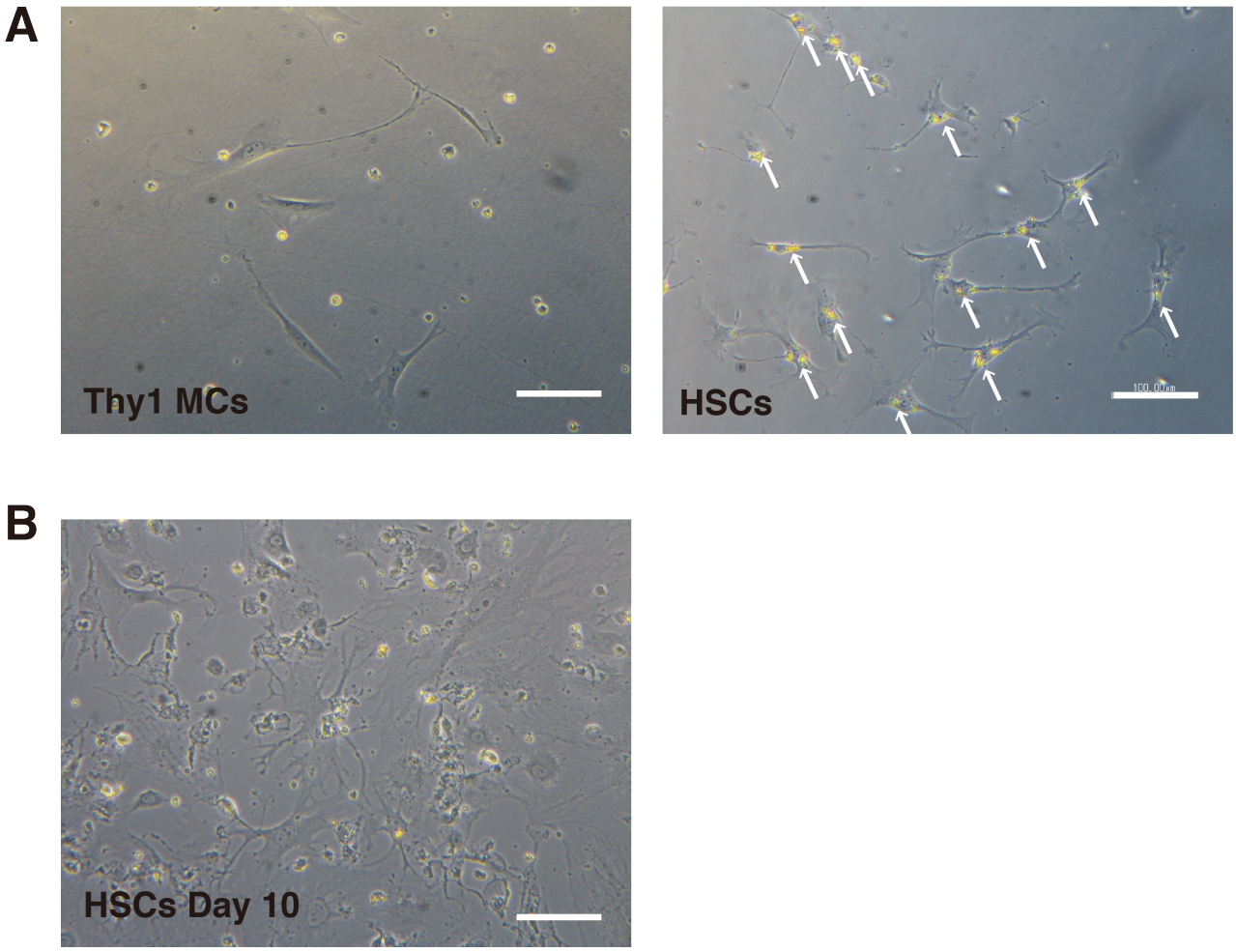

Figure 13. Morphology of cultured Thy1 MCs and HSCs

(A) Phase contrast images of Thy1 MCs (left panel) and HSCs (right panel). Arrows indicate vitamin A-containing lipid droplets. (B) Phase contrast image of HSCs cultured for 10 days. HSCs lost their signature lipid droplets, showed gradual spreading of cytoplasm and filamentous structures appeared. Scale bars = 100 μm.

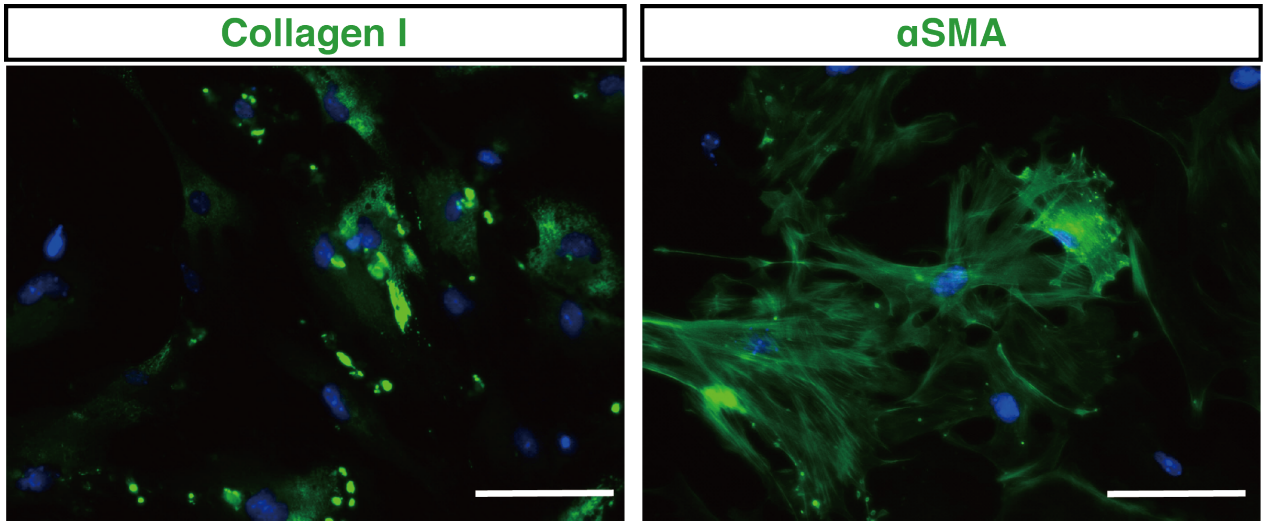

Figure 14. Expression of myofibroblast markers in cultured HSCs

Immunofluorescent staining of collagen type I (green, left panel) and αSMA (green, right panel). Cultured HSCs expressed markers of myofibroblasts, shown by their expression of Collagen I and αSMA. Nuclei were counterstained with Hoechst 33342. Scale bars = 100 μm.

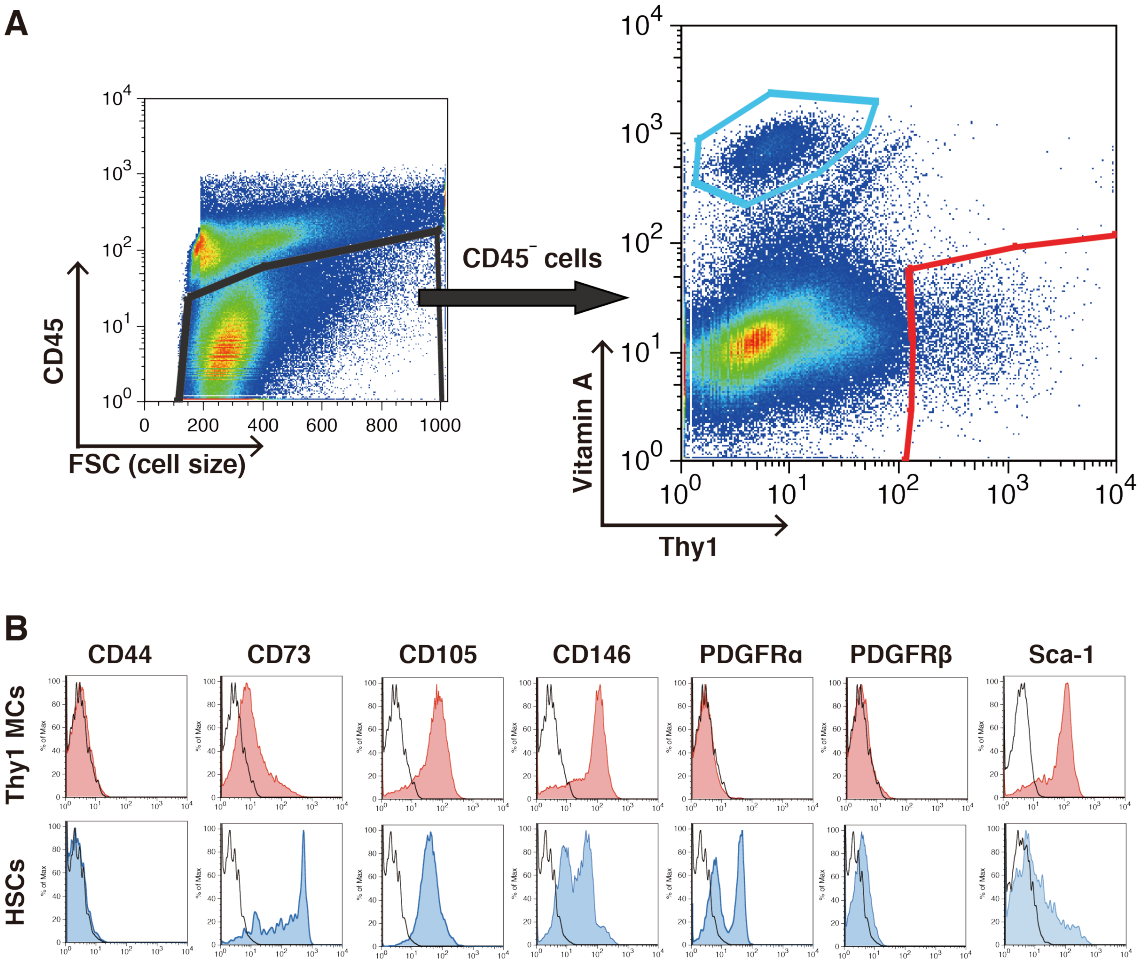

Figure 15. Comparative analysis of Thy1 MCs and HSCs by flow cytometry of NPCs from normal liver

(A) Flow cytometry analysis of NPCs of normal mouse liver. $CD45^+$ leukocytes were excluded from the analysis to directly compare vitamin A autofluorescence and Thy1 expression. FSC reflects cell size. Vitamin A-storing HSCs are represented by blue gate and Thy1 MCs are represented by red gate. Representative dot plot is shown. (B) Thy1 MCs and HSCs were further characterized by the expression of indicated surface markers by histogram plots. Red shaded lines indicate Thy1 MCs, and blue shaded lines indicate HSCs. Black lines indicate isotype control of the corresponding cell types. Abbreviation: FSC, forward scatter.

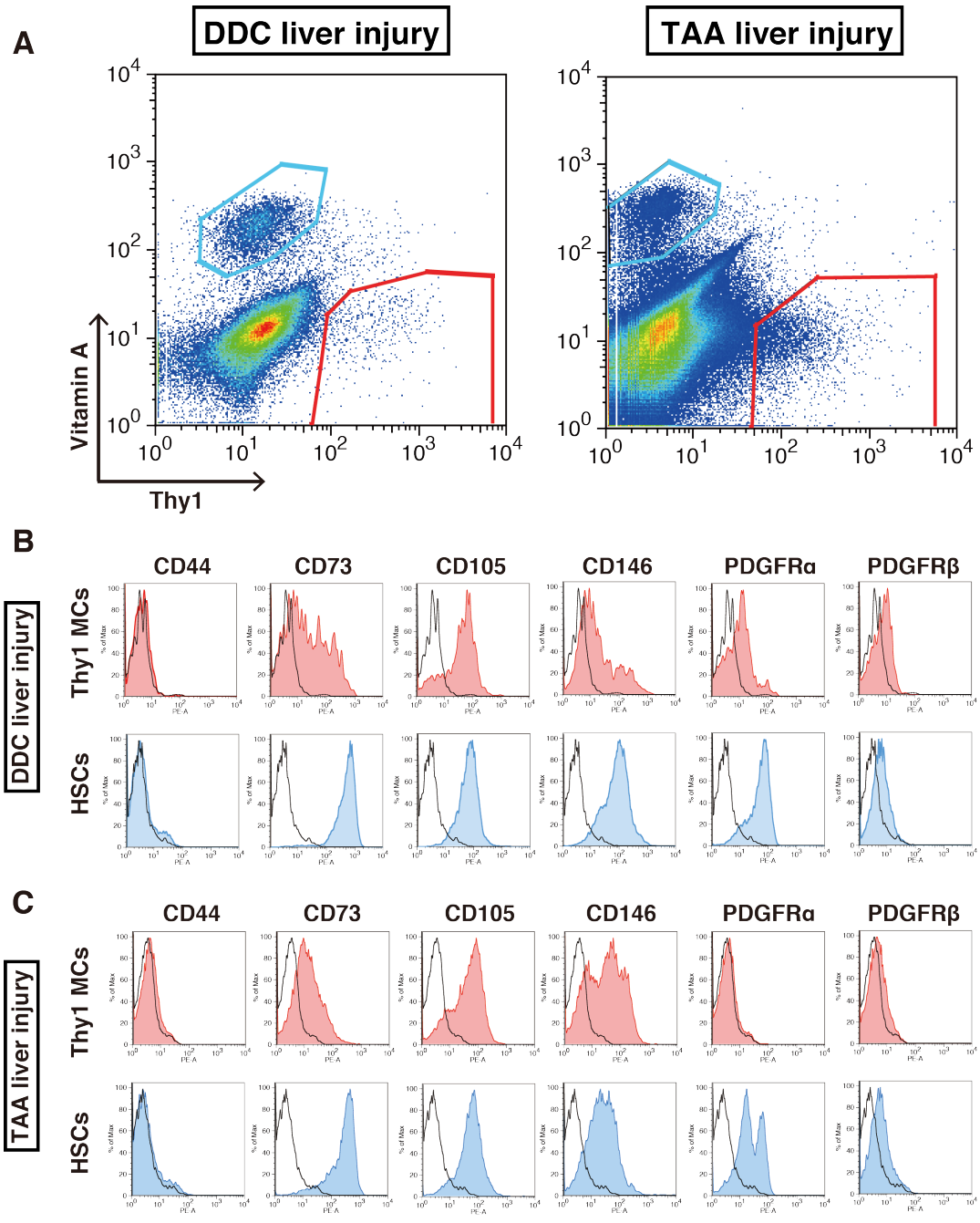

Figure 16. Comparative analysis of Thy1 MCs and HSCs by flow cytometry of NPCs from DDC and TAA injured livers

(A) Flow cytometry analaysis of NPCs of DDC and TAA injured livers. Vitamin A-storing HSCs are represented by blue gate and Thy1 MCs are represented by red gate. (B) Thy1 MCs and HSCs were further characterized by the expression of indicated surface markers by histogram plots. Red shaded lines indicate Thy1 MCs and blue shaded lines indicate HSCs. Black lines indicate isotype control of the corresponding cell types.

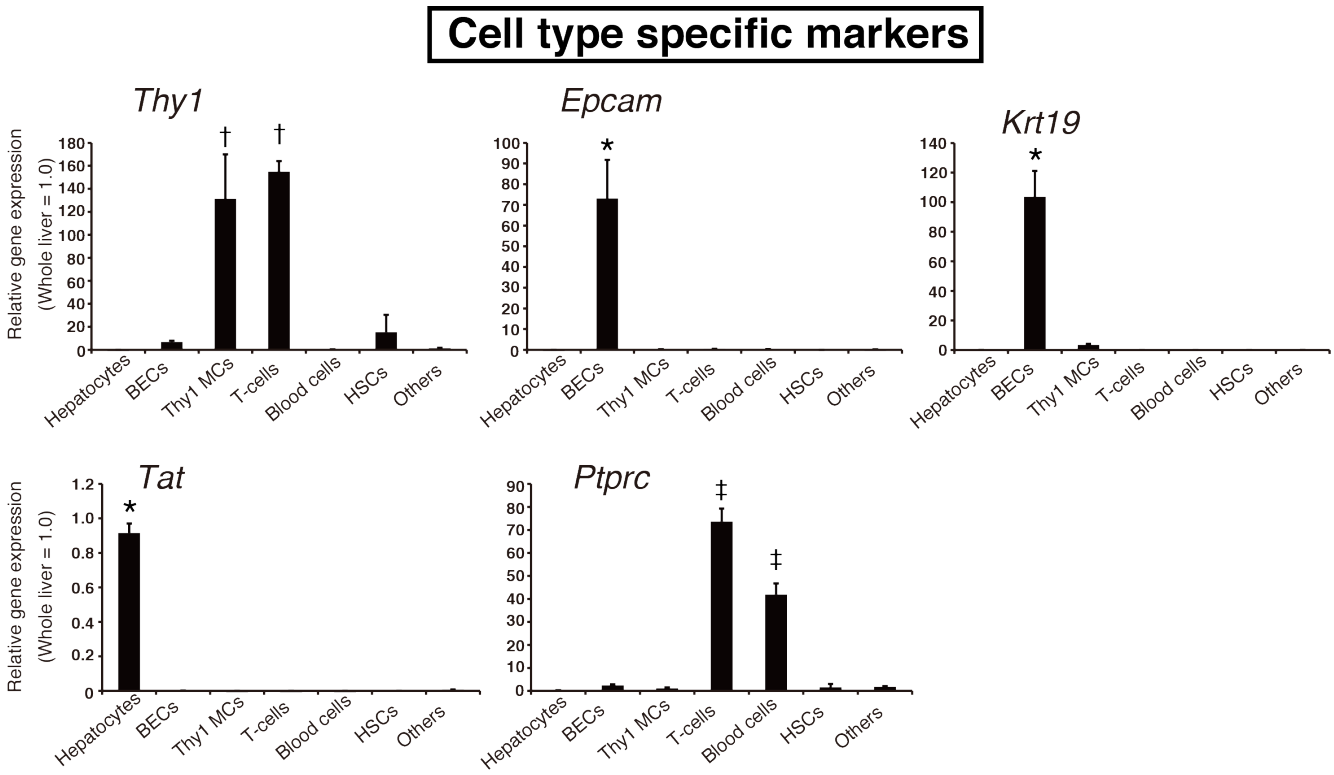

Figure 17. Gene expression analysis of cell type specific markers

Gene expression analysis by quantitative RT-PCR of indicated cell type specific maker genes to confirm specific and adequate isolation of each cell population. *Krt19* (CK19), *Tat* (tyrosine aminotransferase), *Ptprc* (CD45) were used as markers for BECs, hepatocytes, and leukocytes, respectively. Hepatocytes, BECs [EpCAM$^+$ Thy1$^-$ CD45$^-$], Thy1 MCs [EpCAM$^-$ Thy1$^+$ CD45$^-$], T-cells [EpCAM$^-$ Thy1$^+$ CD45$^+$], Blood cells [EpCAM$^-$ Thy1$^-$ CD45$^+$], HSCs [EpCAM$^-$ Thy1$^-$ CD45$^-$ Vitamin A$^+$], and Others [EpCAM$^-$ Thy1$^-$ CD45$^-$ Vitamin A$^-$] cell fractions were isolated from enzymatically digested normal mouse liver of three independent isolations. Expression level of each gene is shown relative to the expression level of normal whole liver sample as 1.0. All gene expression was normalized with β–actin expression. Error bars represent SEM. Statistical analysis was performed using one-way ANOVA, and Tukey as post hoc test. *, significantly different from each of the other 6 fractions ($P < 0.05$); †, significantly different from Hepatocytes, BECs, Blood cells, HSCs and Others ($P < 0.05$); ‡, significantly different from Hepatocytes, BECs, Thy1 MCs, HSCs and Others ($P<0.05$). Abbreviations: Thy1 MCs, Thy1 mesenchymal cells; BECs, biliary epithelial cells; HSCs, hepatic stellate cells.

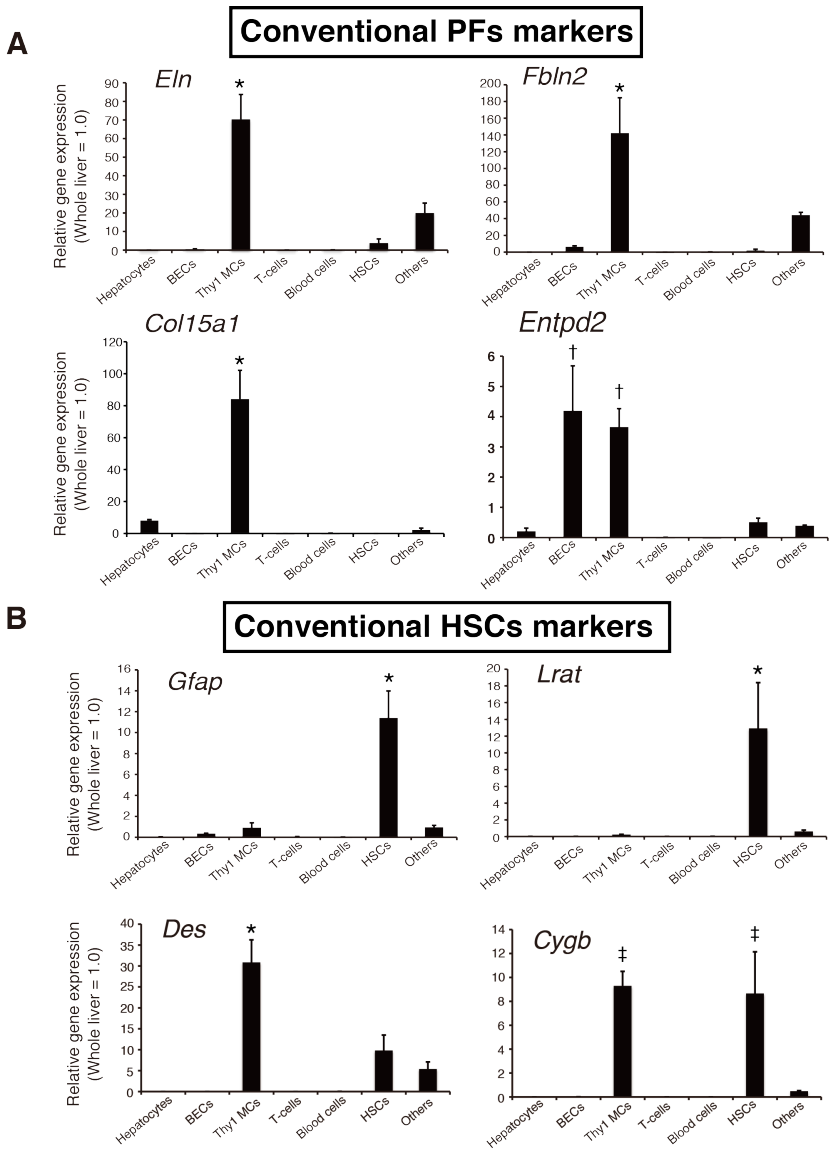

Figure 18. Gene expression analysis of PFs and HSCs signature genes

Gene expression analysis by quantitative RT-PCR of indicated cell type specific maker genes. Hepatocytes, BECs [EpCAM$^+$ Thy1$^-$ CD45$^-$], Thy1 MCs [EpCAM$^-$ Thy1$^+$ CD45$^-$], T-cells [EpCAM$^-$ Thy1$^+$ CD45$^+$], Blood cells [EpCAM$^-$ Thy1$^-$ CD45$^+$], HSCs [EpCAM$^-$ Thy1$^-$ CD45$^-$ Vitamin A$^+$], and Others [EpCAM$^-$ Thy1$^-$ CD45$^-$ Vitamin A$^-$] cell fractions were isolated from enzymatically digested normal mouse liver of three independent isolations. Expression level of each gene is shown relative to the expression level of normal whole liver sample as 1.0. All gene expression was normalized with β–actin expression. Error bars represent SEM. Statistical analysis was performed using one-way ANOVA, and Tukey as post hoc test. *, significantly different from each of the other 6 fractions ($P < 0.05$); †, significantly different from Hepatocytes, T-cells, Blood cells, HSCs and Others ($P < 0.05$); ‡, significantly different from Hepatocytes, BECs, T-cells, Blood cells and Others ($P<0.05$). Abbreviations: Thy1 MCs, Thy1 mesenchymal cells; BECs, biliary epithelial cells; HSCs, hepatic stellate cells.

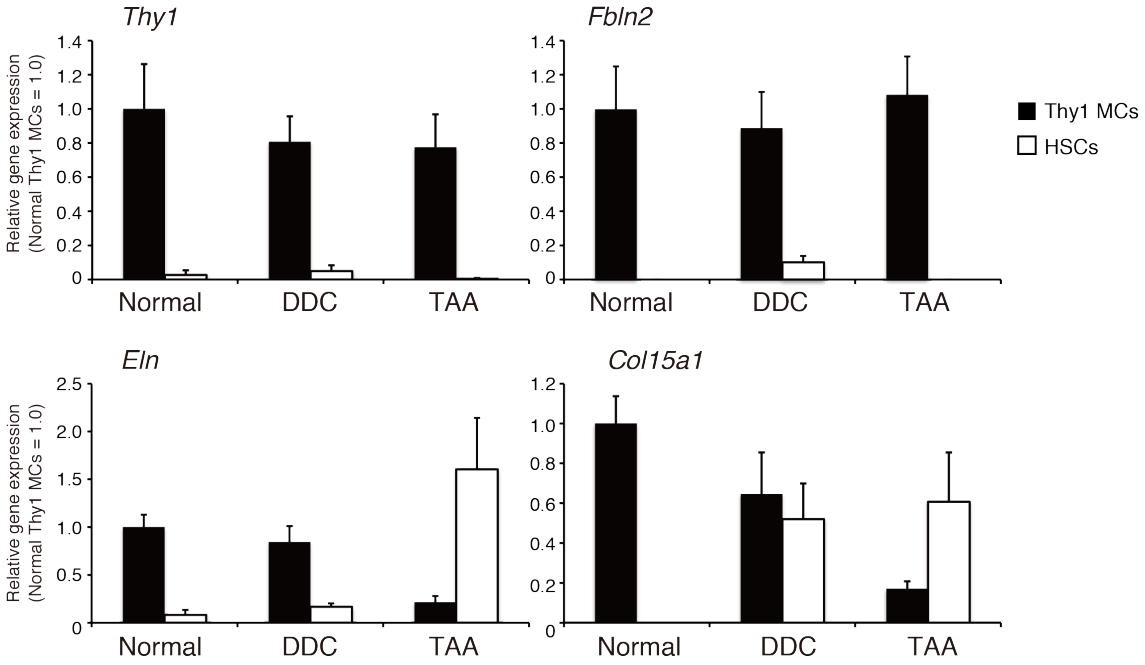

Figure 19. Expression changes of PFs markers upon liver injury

Comparative gene expression changes of PFs markers among Thy1 MCs and HSCs isolated from normal, DDC- and TAA-injured livers. Black bars indicate Thy1 MCs and white bars indicate HSCs. Expression level of each gene in Thy1 MCs isolated from normal liver is shown to be 1.0. All gene expression was normalized with β–actin expression. Error bars represent SEM.

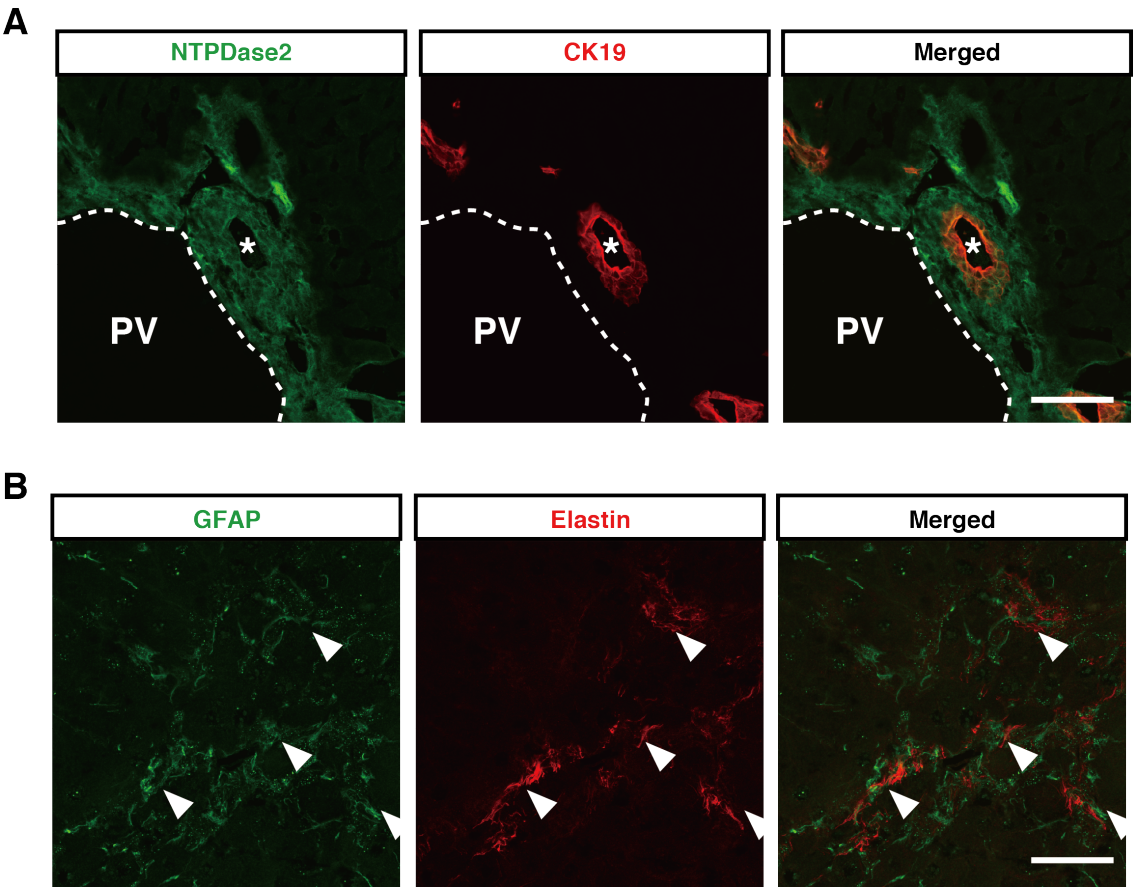

Figure 20. Expression of some PFs markers by other cell types

(A) Immunofluorescent staining of NTPDase2 (green) and CK19 (red) in normal mouse liver tissue section. PV is shown in white dotted lines. Asterisk indicates bile duct. (B) Immunofluorescent staining of GFAP (green) and elastin (red) in TAA-injured mouse liver tissue section. Arrowheads indicate elastin expression located in proximity to GFAP-expressing HSCs. Scale bars = 50 μm. Abbreviation: PV, portal vein.

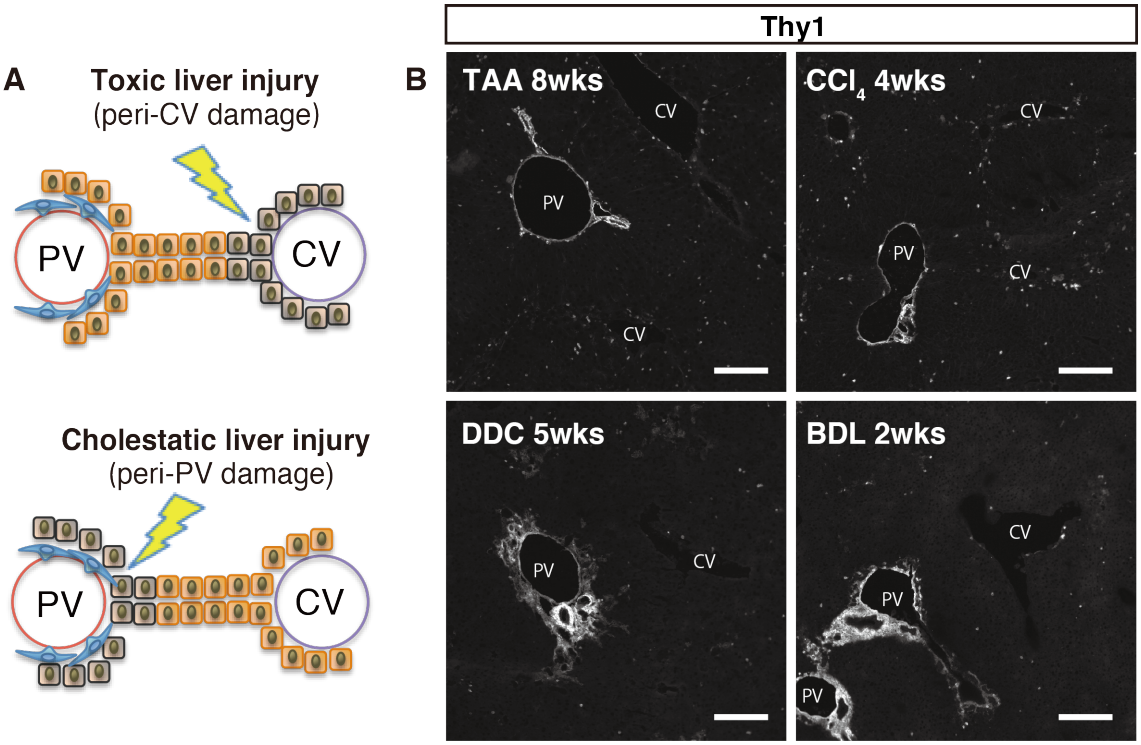

Figure 21. Analysis of Thy1-expressing cells in different types of injuries

(A) Schematic diagram of different types of liver injuries. Toxic liver injury models, such as TAA- and CCl_4-induced liver injury, causes hepatocellular damage in the central vein area (upper panel). Cholestatic liver injury models, such as DDC- and BDL-induced liver injury, causes damage in the peri-portal area. (B) Immunostaining of Thy1 shown in gray scale, in liver tissue sections of each indicated liver injury models. Scale bars = 200 μm. Abbreviations: CV, central vein; PV, portal vein.

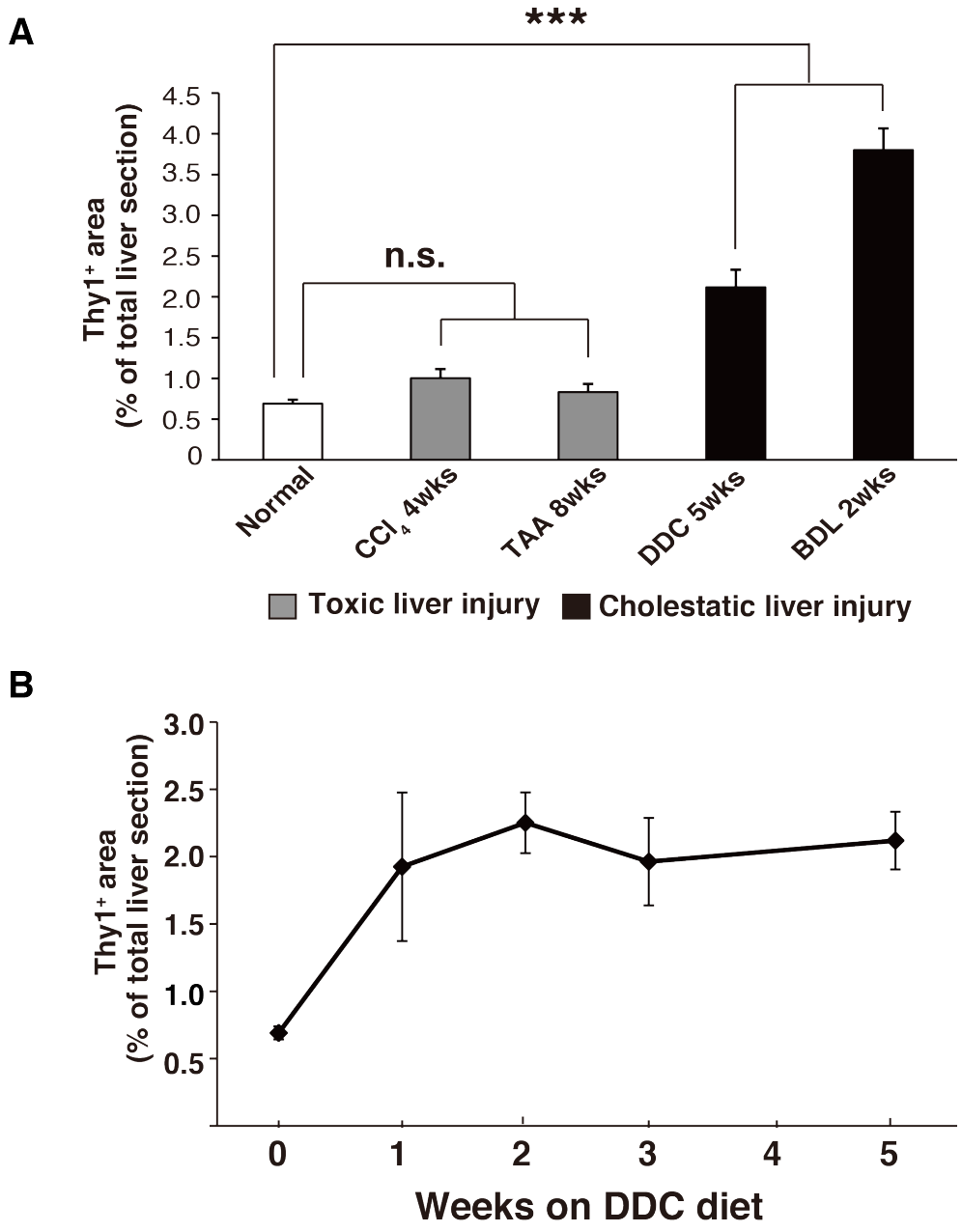

Figure 22. Quantification of Thy1 area in liver tissue sections

(A) Whole liver tissue sections of each indicated liver injury models have been stained with Thy1, and Thy1 positive area was quantified using the IN Cell Analyzer 2000. T-lymphocytes were removed from the area quantification by kernel size selection. Statistical analysis was performed using one-way ANOVA, and Dunnett as post hoc test. Error bars indicate SEM. ***$P < 0.001$; n.s., no significance, compared to normal liver. (B) Thy1 positive area was quantified in liver tissue sections of mice fed with DDC diet for the indicated time points. $Thy1^+$ area increased upon DDC-induced liver injury. All areas were quantified on 3 biological replicates of each liver injury models.

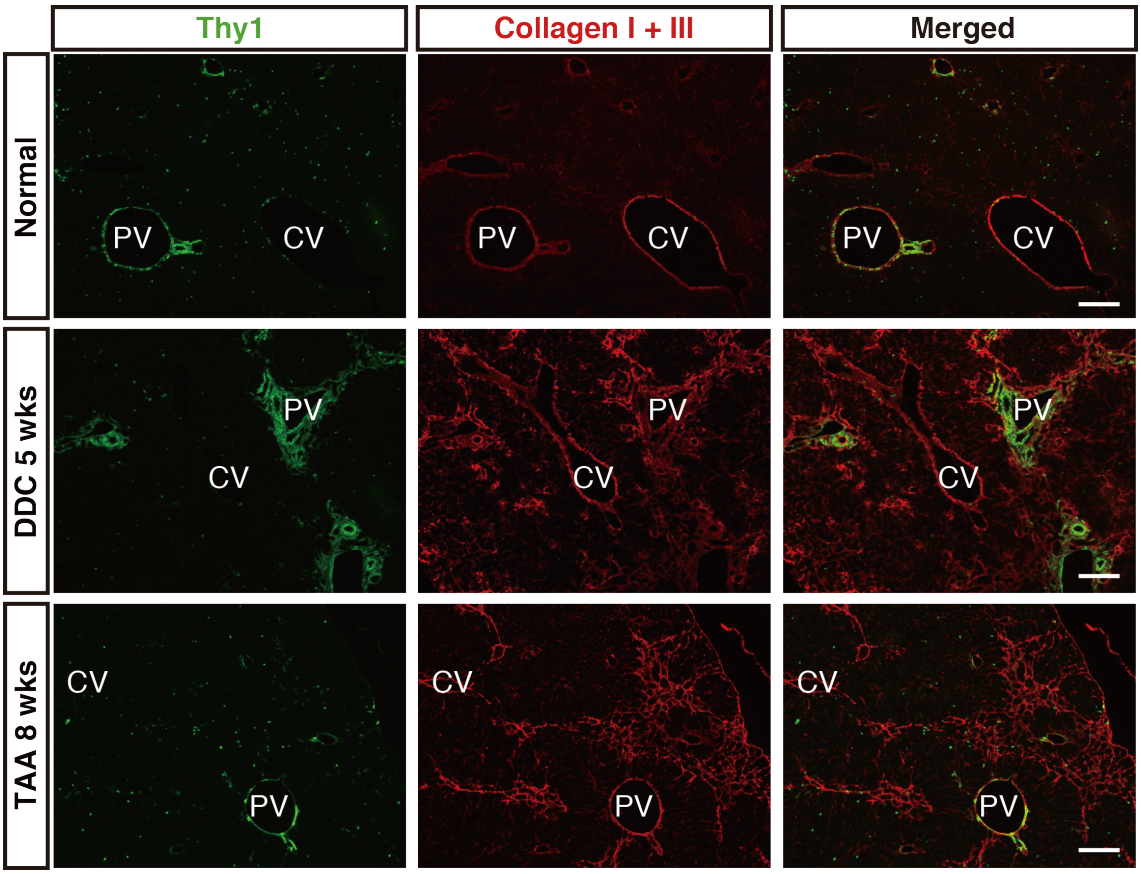

Figure 23. Anatomical location of Thy1-expressing cells and positional relation to collagen accumulation upon chronic liver injury

Immunofluorescent staining of Thy1 (green) and type I and III collagen (red) in liver tissue sections of normal, DDC- and TAA-injured livers. Scale bars = 200 μm. Abbreviations: CV, central vein; PV, portal vein.

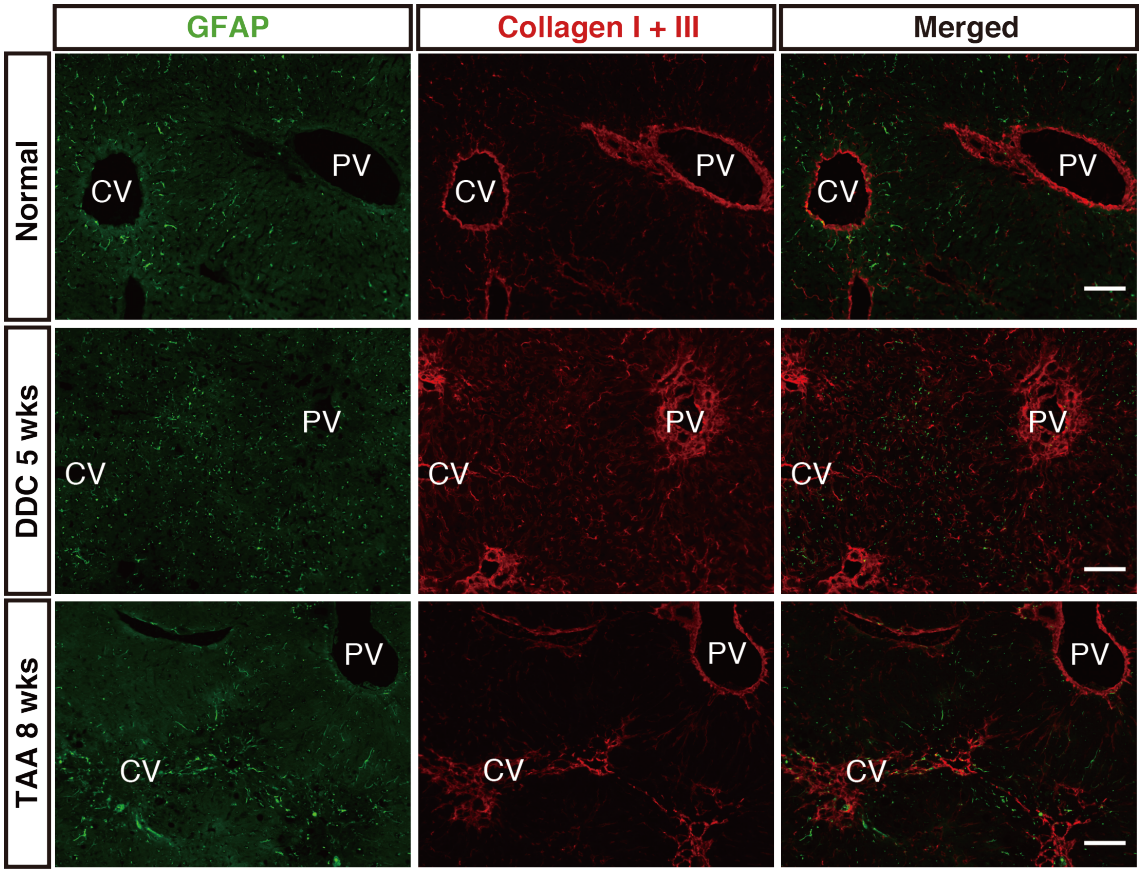

Figure 24. Anatomical location of GFAP-expressing HSCs and positional relation to collagen accumulation upon chronic liver injury

Immunofluorescent staining of GFAP (green) and type I and III collagen (red) in liver tissue sections of normal, DDC- and TAA-injured livers. Scale bars = 200 μm. Abbreviations: CV, central vein; PV, portal vein.

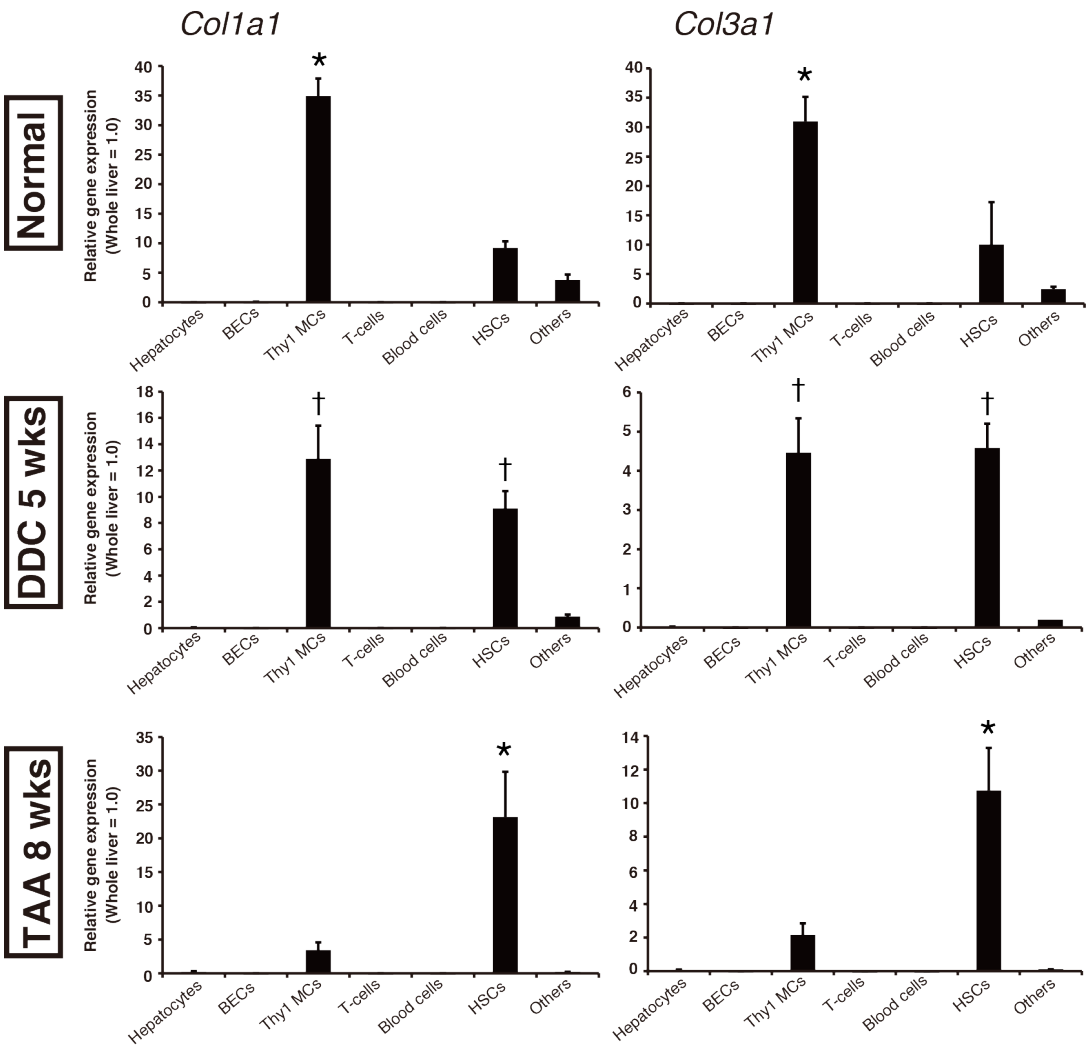

Figure 25. Gene expression analysis of fibrogenic genes

Gene expression analysis by quantitative RT-PCR in each liver cell fraction isolated from mice fed with normal diet and normal water, mice fed with DDC diet for 5 weeks, or mice administered with TAA drinking water for 8 weeks. Expression level of each gene is shown relative to the expression level of the corresponding whole liver sample as 1.0. All gene expression was normalized with β–actin expression. Error bars indicate SEM. Statistical analysis was performed using one-way ANOVA, and Tukey as post hoc test. *, significantly different from each of the other 6 fractions ($P < 0.05$); †, significantly different from Hepatocytes, BECs, T-cells, Blood cells and Others ($P < 0.05$).

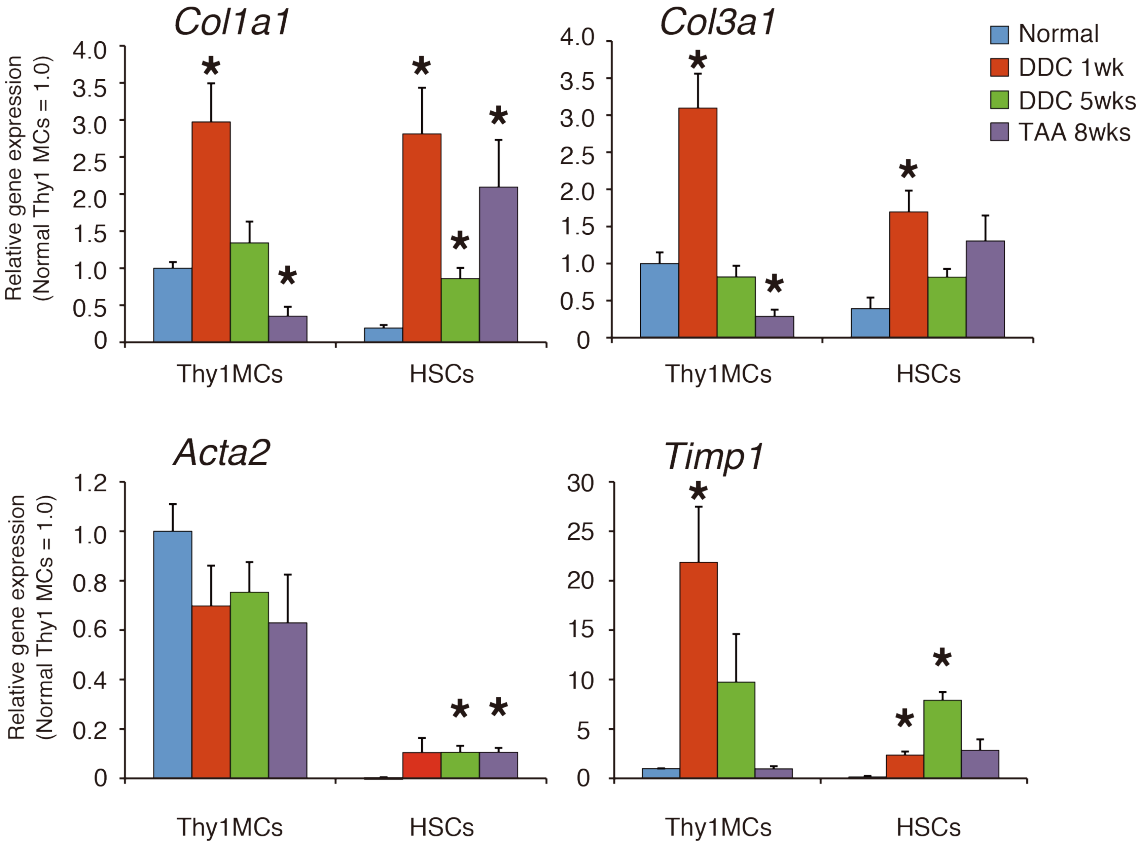

Figure 26. Comparative gene expression analysis of fibrogenic genes in Thy1 MCs and HSCs from normal and injured livers

Gene expression analysis by quantitative RT-PCR of Thy1 MCs and HSCs isolated from mice fed with normal diet and normal drinking water, mice fed with DDC diet for 1 week or 5 weeks, and mice administered with TAA drinking water for 8 weeks (n = 3 independent isolations). Expression level of each gene is shown relative to the expression level of normal whole liver sample as 1.0. All gene expression was normalized with β–actin expression. Error bars indicate SEM. Statistical analysis was performed using two-tailed Student's *t* test. *, significantly different compared to normal condition ($P < 0.05$).

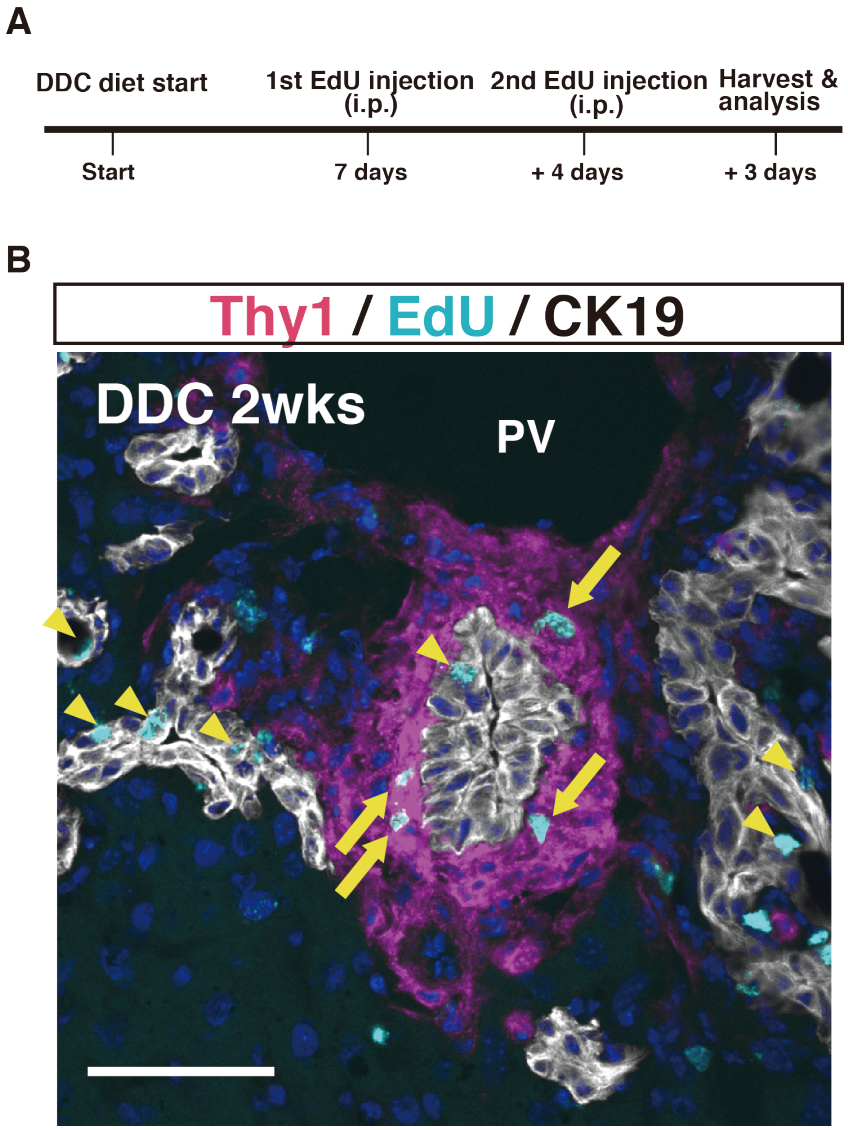

Figure 27. EdU incorporation by Thy1-expressing cells upon DDC-induced cholestatic liver injury

(A) Experimental scheme of EdU injection. Mice were injected with EdU (50 μg/g body weight) intraperitoneally at the indicated time points prior to analysis. (B) Fluorescent staining of Thy1 (magenta) and EdU (cyan) in DDC injured liver section. Arrows indicate EdU positive Thy1-expressing cells. Arrowheads indicate EdU positive cells among the $CK19^{+}$ biliary epithelial cells. Nuclei are shown in blue. Scale bar = 50 μm. Abbreviation: PV, portal vein.

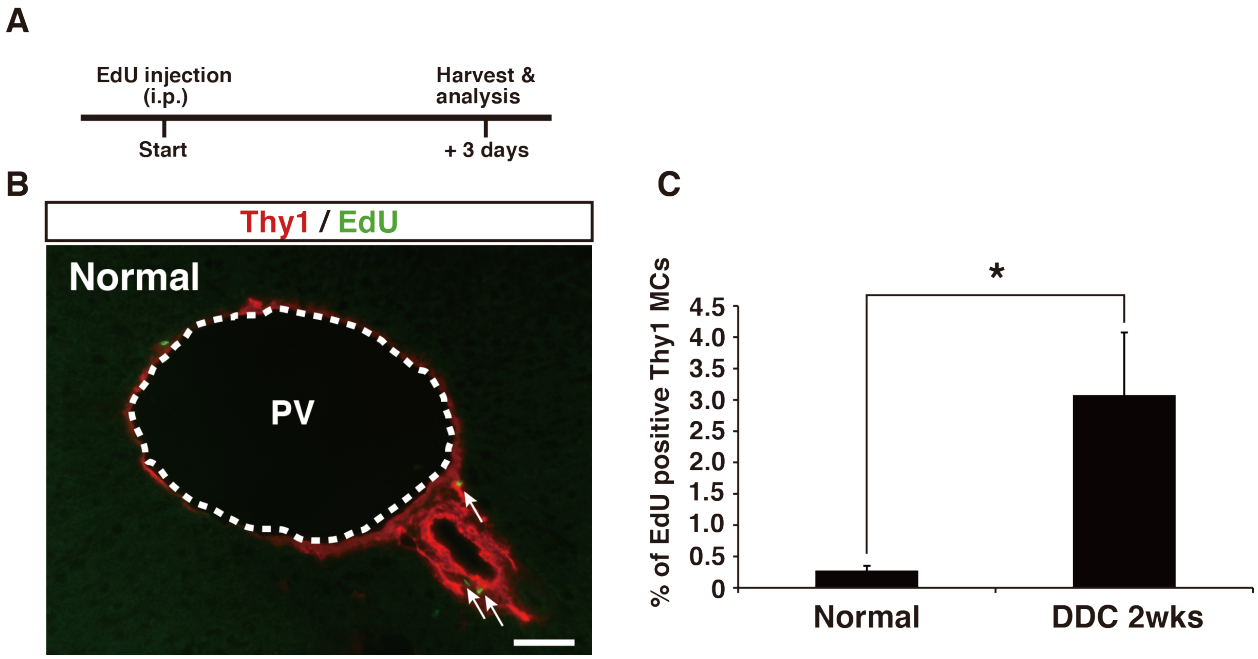

Figure 28. Incorporation of EdU in normal liver and quantification of EdU incorporation by Thy1 MCs

(A) Experimental scheme of EdU injection. Mice were injected with EdU (50 μg/g body weight) intraperitoneally prior to analysis. (B) Fluorescent staining of Thy1 (red) and EdU (green) in normal mouse liver tissue section. Scale bars = 50 μm. (C) Quantification of EdU positive Thy1 MCs by flow cytometry, in cells isolated from mice fed with either normal or DDC diet. Analysis was performed in 3 biological replicates. Error bars indicate SEM. Statistical analysis was performed using two-tailed Student's *t* test. *, significantly different compared to normal condition ($P < 0.05$).

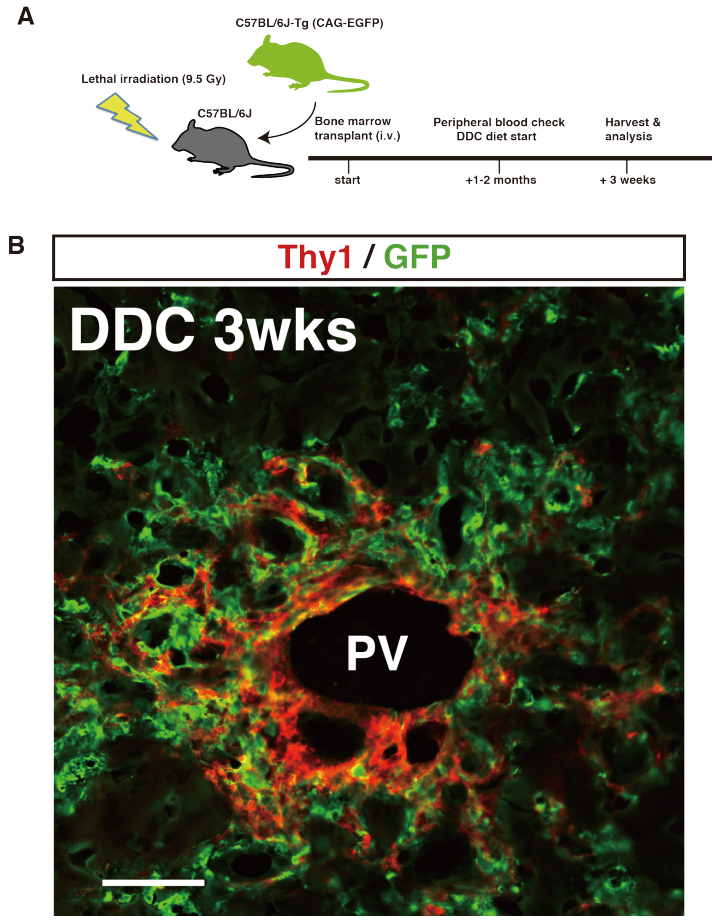

Figure 29. Infiltration of bone marrow-derived Thy1-expressing cells upon DDC-induced liver injury

(A) Experimental scheme of whole bone marrow transplant. (B) Immunostaining of Thy1 (red) and GFP (green) in transplanted mice fed with DDC. Left panel shows image of low magnification. Scale bar = 50 μm. Right panel shows highly magnified image of area surrounded by the white box. Scale bar = 10 μm. Nuclei were counterstained with Hoechst 33342. Arrowheads indicate GFP positive Thy1-expressing cells. Abbreviations: i.v., intravenous injection; PV, portal vein.

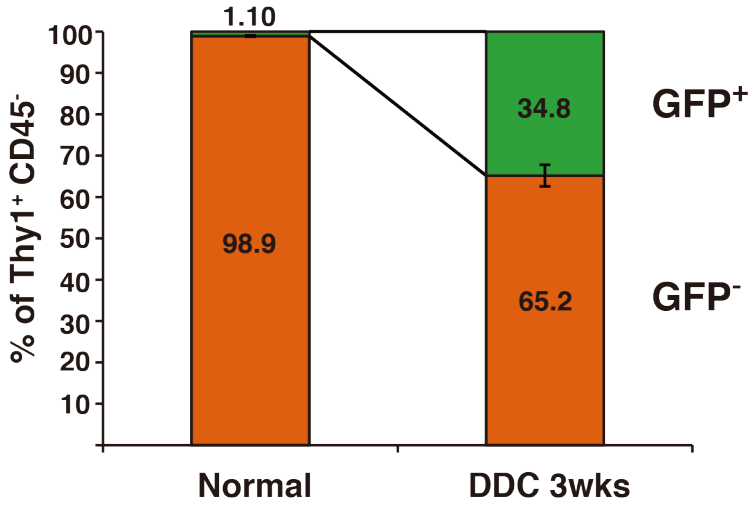

Figure 30. Quantification of GFP positive cells in Thy1 MCs

Quantification of GFP positive Thy1 MCs ($Thy1^+$ $CD45^-$) by flow cytometry, in cells isolated from transplanted mice fed with either normal or DDC diet. Green bars indicate GFP positive Thy1 MCs, and orange bars indicate GFP negative Thy1 MCs. Analysis was performed in 3 biological replicates. Error bars indicate SEM.

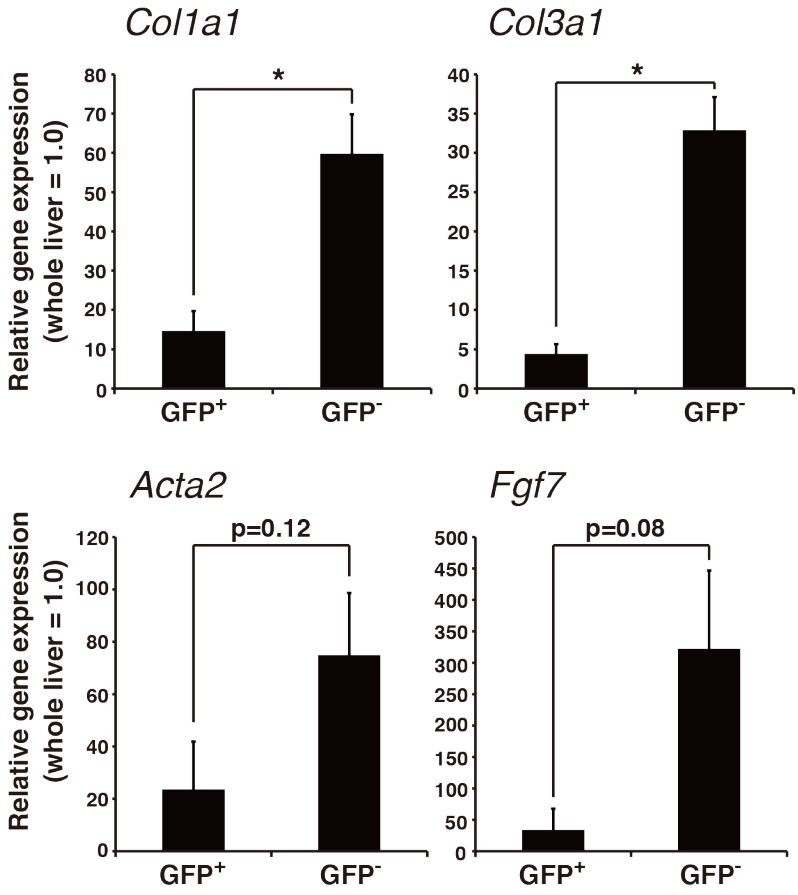

Figure 31. Gene expression analysis of fibrogenic genes

Gene expression analysis by quantitative RT-PCR of GFP$^+$ Thy1$^+$ CD45$^-$ and GFP$^-$ Thy1$^+$ CD45$^-$ cells (n = 3 or independent isolations). Expression level of each gene is shown relative to the expression level of normal whole liver sample as 1.0. All gene expression was normalized with β–actin expression. Error bars indicate SEM. *$P < 0.05$, as calculated by two-tailed Student's t test.

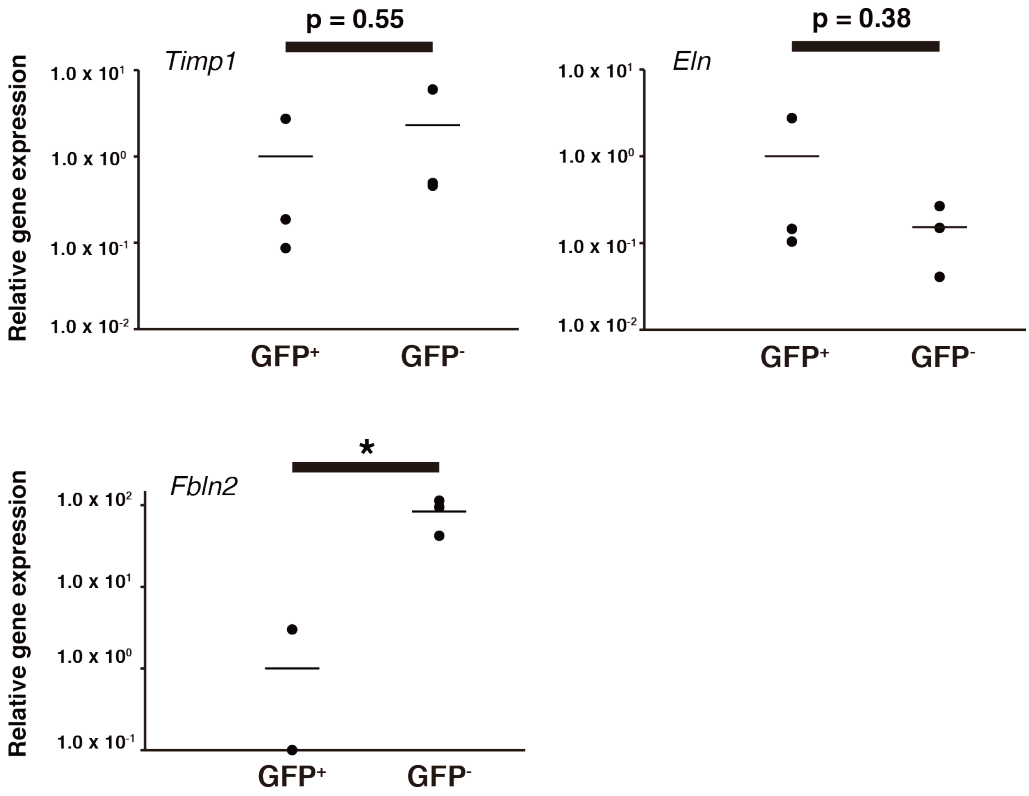

Figure 32. Gene expression analysis of characteristic PF markers

Gene expression analysis by quantitative RT-PCR of GFP$^+$ Thy1$^+$ CD45$^-$ and GFP$^-$ Thy1$^+$ CD45$^-$ cells (n = 3 or independent isolations) shown as dot plots. Horizontal lines indicate average expressions. All gene expression was normalized with β–actin expression. $^*P < 0.05$, as calculated by two-tailed Student's *t* test.

Table 1. List of antibodies used in the study

Antibody	Host	Application	Dilution	Supplier; Cat No. / Clone
Thy1.2	Rat	FCM, IHC	1:100	BD biosciences, San Diego CA; 30H12
CD31	Rabbit	IHC	1:200	NeoMarkers, Fremont CA; RB-10333-P0
Desmin	Rabbit	IHC	1:100	Abcam, Cambridge UK; ab8592
Elastin	Rabbit	IHC	1:100	Cedarlane, Ontario Canada; CL55041AP
EpCAM	Rat	FCM	1:100	Okabe et al. 2009
CD45	Rat	FCM, IHC	1:100	Biolegend, San Diego CA; 30-F11
CD3ε	Armenian hamster	FCM	1:100	Biolegend, San Diego CA; 145-2C11
TCR ß chain	Hamster	FCM	1:100	Pharmingen, San Diego CA; H57-597
Collagen type I	Rabbit	IHC, ICC	1:100	AbD Serotec, Hercules CA; 2150-1410
Collagen type III	Rabbit	IHC, ICC	1:300	Abcam, Cambridge UK; ab7778
αSMA	Rabbit	IHC, ICC	1:100	Abcam, Cambridge UK; ab5694

CD44	Rat	FCM	1:100	Biolegend, San Diego CA; IM7
CD73	Rat	FCM	1:100	Biolegend, San Diego CA; TY/11.8
CD105	Rat	FCM	1:100	eBioscience, San Diego CA; MJ7/18
CD140b	Rat	FCM	1:100	Biolegend, San Diego CA; APB5
CD146	Rat	FCM	1:100	Biolegend, San Diego CA; ME-9F1
Sca-1	Rat	FCM	1:100	Pharmingen, San Diego CA; E13-161.7
NTPDase2	Sheep	IHC	1:100	R&D systems, Minneapolis MN; AF5797
GFAP	Goat	IHC	1:100	Abcam, Cambridge UK; ab53554
GFP	Rabbit	IHC	1:100	MBL, Nagoya JPN; 598

Table 2. List of oligonucleotide primers used for qPCR analysis

Gene name	Direction	Sequence (5' to 3')
Acta2 (αSMA)	Fwd	GACACCACCCACCCAGAGT
	Rev	ACATAGCTGGAGCAGCGTCT
Col1a1	Fwd	CATGTTCAGCTTTGTGGACCT
	Rev	GCAGCTGACTTCAGGGA TGT
Col3a1	Fwd	TCCCCTGGAATCTGTGAATC
	Rev	TGAGTCGAATTGGGGAGAAT
Col15a1	Fwd	GCCCCCTACTTCATCCTCTC
	Rev	CAGTACGGACCTCCAGGGTA
Cygb	Fwd	CCGGGCGACATGGAGATAG
	Rev	GTCCTCGCAGTTGGCATAC
Des	Fwd	GTGGATGCAGCCACTCTAG
	Rev	TTAGCCGCGATGGTCTCAT
Eln	Fwd	TTGCTGATCCTCTTGCTCA
	Rev	GCCCCTGGATAATAGACTC
Entpd2	Fwd	ATGGCTGGAAAGTTGGTGTCA
	Rev	TCTTGGGTAGGGACGCACA
Epcam	Fwd	AGGGGCGA TCCAGAACAACG
	Rev	ATGGTCGTAGGGGCTTTCTC
Fbln2	Fwd	TGTTGTTGGGGACACAGCTA

	Rev	CCATCAAACACTCGTCTTGGT
Fgf7	Fwd	TTTGGAAAGAGCGACGACTT
	Rev	GGCAGGATCCGTGTCAGTAT
Gfap	Fwd	ACAGACTTTCTCCAACCTCCAG
	Rev	CCTTCTGACACGGATTTGGT
Krt19	Fwd	CCGGACCCTCCCGAGA TTA
	Rev	CTCCACGCTCAGACGCAAG
Lrat	Fwd	CTAATCCCAAGACAGCCGAA
	Rev	TATGGCTCTCGGATCAGTCC
Ptprc (CD45)	Fwd	GAGGTGTCTGATGGTGCAAG
	Rev	TGTATTCCACTAAAGCCTGATGAA
Tat	Fwd	CATCTGGAGCCATGTACCTT
	Rev	TCCAGCA TCA TCACCTCG
Timp1	Fwd	GCAAAGAGCTTTCTCAAAGACC
	Rev	AGGGATAGATAAACAGGGAAACACT
Thy1	Fwd	GAAAACTGCGGGCTTCAG
	Rev	CCAAGAGTTCCGACTTGGAT
Vim	Fwd	CGGCTGCGAGAGAAATTGC
	Rev	CCACTTTCCGTTCAAGGTCAAG
Actb	Fwd	CCAACCGTGAAAAGATGACC
	Rev	CCAGAGGCATACAGGGACAG

Acknowledgment

The present study was performed under the supervision of Professor A. Miyajima and Associate Professor T. Itoh. I would like to hereby express my special appreciation to their strict mentorship and long support, which made possible for this research to be accomplished.

Special thanks go to N. Miyata and C. Koga for cell sorting, N. Imaizumi for animal care, and the members of the Miyajima lab for helpful discussions and advice.

Lastly, I would like to thank my parents, for their love since the very first day of my life, and for their support from overseas, both spiritually and financially, since the day when I came to Japan by myself. This journey was never easy to take on my own, but your love and support has got me keep on rowing to move forward and strive for the goal until the end.